Journal of Catalysis 456 (2026) 116721

Contents lists available at ScienceDirect

Journal of Catalysis

journal homepage: www.elsevier.com/locate/jcat

Research article

# Mechanistic Insights on the β-(*Z*) alkyne hydrosilylation by a NHC-based Cp*Rh(III) catalyst: from catalyst design to an alternative model for H-Si activation

Isabel Poves-Ruiz [a], Beatriz Sánchez-Page [a], M. Victoria Jiménez [a,*], Miguel Gallegos [b], Julen Munarriz [c], Vincenzo Passarelli [a], Jesús J. Pérez-Torrente [a,*]

[a] Departamento de Química Inorgánica, Instituto de Síntesis Química y Catálisis Homogénea-ISQCH, Universidad de Zaragoza-C.S.I.C., 50009 Zaragoza, Spain
[b] Departamento de Química Física y Analítica. Universidad de Oviedo, 33006 Oviedo, Spain
[c] Departamento de Química Física and Instituto de Biocomputación y Física de Sistemas Complejos, Universidad de Zaragoza 50009 Zaragoza, Spain

ARTICLE INFO

*Keywords:*
Hydrosilylation
Alkynes
Reaction mechanisms
Rhodium
N-heterocyclic carbenes

ABSTRACT

In-depth studies on the residual hydrosilylation catalytic activity of samples of compound [Cp*RhI{(MeIm)$_2$CH$_2$}]$^+$, bearing an unfunctionalized bis-NHC ligand, lead to the discovery of the excellent catalytic performance of the simple complex [Cp*RhI$_2$(IMe)] (IMe = 1,3-dimethylimidozol-2-ylidene). This compound efficiently catalyzes the hydrosilylation of wide a range of terminal alkynes, with complete regio- and stereoselectivity toward the thermodynamically less stable β-(Z)-vinylsilane isomer. The reaction mechanism has been explored by DFT calculations. The reaction seems to proceed through an ionic outer-sphere mechanism, involving heterolytic activation of the hydrosilane assisted by the rhodium center and a solvent molecule (acetone). In the absence of acetone, a metal–ligand cooperation reaction pathway is proposed, in which the Cp* ligand acts as a proton-relay within the coordination sphere of the Rh(III) center. The cooperative activation of the hydrosilane by the metallocene moiety of the catalyst precursor generates a reactive Rh(I)–silyl intermediate bearing a pentamethylcyclopenta-1,3-diene ligand, [η$^4$-Cp*H], formed through protonation of the Cp* moiety.

## 1. Introduction

Organosilicon compounds play a pivotal role in diverse fields such as materials science, medicinal chemistry, and synthetic organic chemistry. [1] Although numerous methods have been developed for the synthesis of organosilicon compounds with potentially useful properties, the hydrosilylation of unsaturated bonds, such as alkenes and alkynes, has become a major atom-economic transformation to prepare silicon-containing organic compounds. [2] In particular, vinylsilanes are valuable building blocks to access value-added functional hydrocarbons due to their versatility to transform into other functional groups, excellent stability, low toxicity, and simplicity of handling relative to other vinyl-metal species. [3].

Among the available synthetic approaches, the transition metal-catalyzed hydrosilylation of alkynes stands out as one of the most straightforward and atom-economical method for the preparation of vinylsilanes. [4] However, the hydrosilylation of terminal alkynes can afford three vinylsilanes isomers, namely α, β-(*Z*) and β-(*E*), and thus, precise control over the regioselectivity (α- or β-selectivity), and stereoselectivity (syn- or anti-selectivity) of the reaction remains a significant challenge (Scheme 1). [5] Moreover, alkyne dehydrosilylation, reduction, or dihydrosilylation, and isomerization processes are also competitive side reactions. [6].

Significant progress has been made in the development of transition metal catalysts to address challenges associated with selectivity. In particular, there has been growing interest in the design of NHC-based alkyne hydrosilylation catalysts based on both noble metals [7] and earth-abundant metals [8] to control both regioselectivity and stereoselectivity. NHC–Pt(0) catalysts developed by Markó preferentially afford the β-(*E*)-vinylsilane isomer in the hydrosilylation of terminal alkynes. [9] In contrast, a preference for the thermodynamically unfavorable β-(*Z*)-vinylsilane isomer was found for some NHC–Rh(I) and Ir(I) catalysts, [10] although in some cases β-(*Z*) → β-(*E*) vinylsilane isomerization resulted in a decrease of stereoselectivity. [11] Interestingly, rhodium(I) complexes bearing N-functionalized NHC ligands have been shown to be excellent catalyst precursors for selectively accessing both

* Corresponding authors.
*E-mail addresses:* vjimenez@unizar.es (M.V. Jiménez), perez@unizar.es (J.J. Pérez-Torrente).

https://doi.org/10.1016/j.jcat.2026.116721
Received 12 November 2025; Received in revised form 23 January 2026; Accepted 26 January 2026
Available online 31 January 2026

β-(*E*)-vinylsilanes [12] and β-(*Z*)-vinylsilanes. [13] Additionally, NHC-based bimetallic and multinuclear hydrosilylation catalysts have been reported, albeit with only modest control over reaction selectivity. [14] In this context, a deeper understanding of the reaction mechanisms is pivotal for the rational design of more active and selective catalytic systems with wider applicability.

The hydrosilylation of terminal alkynes usually proceeds with anti-Markovnikov regiochemistry and predominantly *syn*-addition stereochemistry through the well stablished classic inner-sphere Chalk-Harrod mechanism that leads to the β-(*E*)-vinylsilane product. [15] However, the formation of the β-(*Z*)-vinylsilane, the trans addition product, is consistent with a modified Chalk-Harrod mechanism which entails the silylmetalation of the alkyne followed of the metal-assisted isomerization of the resulting (*Z*)-silylvinylene intermediate to the thermodynamically more favorable (*E*)-silylvinylene complex. The isomerization proceeds via a $\eta^2$-vinylsilane or metallacyclopropene intermediate, as proposed in the widely recognized Crabtree–Ojima mechanism. [16] In any case, both mechanisms involve the oxidative addition of the hydrosilane, which is consistent with catalytic cycle proceeding through $Pt^0/Pt^{II}$ or $M^I/M^{III}$ (M = Rh, Ir) intermediates. However, for rhodium(III) and iridium(III) precatalysts, the potential participation of $M^{III}/M^V$ (M = Rh, Ir) intermediates remains a subject of debate. Although experimental evidence has so far proved elusive, [17] several mechanistic proposals have suggested the participation of high-valent Rh(V) and Ir (V) complexes as intermediates in catalytic hydrosilylation reactions of carbonyl compounds and alkenes. [18] Accordingly, the number of reported Rh(III) and Ir(III) catalysts remains limited [19] and alternative mechanistic pathways have been proposed to account for their activity. A representative selection of NHC-Rh(III) catalyst for the hydrosilylation of alkynes is shown in Chart 1 [20].

In this regard, an ionic outer-sphere mechanism for the hydrosilylation of terminal alkynes catalyzed by $[M^{III}(bis\text{-}NHC)I_2]^+$ (M = Ir and Rh) has been proposed. This pathway involves the heterolytic activation of the hydrosilane assisted by the metal center and a molecule of solvent (acetone) that acts as a silane-shuttle. [21] On the other hand, the potential of cyclometalated Rh(III) compounds as precatalyst for hydrosilation reactions has been recognized. In particular, we have shown that the Rh−$C_{Ar}$ bond in the Rh(III)-triazolylidene complex [Cp*RhI(C,C′)-Triaz] is a reactive site involved in the precatalyst activation through reaction with the hydrosilane, leading to the formation of reactive silyl species. [22].

Besides, we have recently reported a zwitterionic compound [Cp*RhCl{(MeIm)$_2$CHCOO}] that proved to be an efficient catalyst for the hydrosilylation of terminal alkynes with excellent regio- and stereoselectivity toward the β-(*Z*)-vinylsilane isomer under mild reaction conditions. Mechanistic investigations suggested an ionic outer-sphere mechanism pathway, in which the carboxylate fragment, which is involved in the activation of the hydrosilane, acts as a silyl carrier. [23] The catalytic inactivity of $[Cp^*RhI\{(MeIm)_2CH_2\}]^+$, a related cationic compound with an unfunctionalized bis-NHC ligand, under the same conditions provided experimental evidence for the key role of the carboxylate function. However, we have observed that compound $[Cp^*RhI\{(MeIm)_2CH_2\}]^+$ has residual alkyne hydrosilylation activity in acetone, showing also excellent β-(*Z*) selectivity.

In this context, the aim of this work is to conduct an in-deep study of the catalytic system based on $[Cp^*RhI\{(MeIm)_2CH_2\}]^+$ to identify the true active species responsible for its catalytic activity in acetone. Experimental studies have led to the characterization of the active species, which has enabled the rational redesign of the catalyst as [Cp*RhI$_2$(IMe)] (IMe = 1,3-dimethylimidozol-2-ylidene). Intriguingly, this catalyst has shown remarkable alkyne hydrosilylation activity in both acetone and chloroform. Mechanistic investigations, supported by DFT calculations, indicate that the reaction proceeds through distinct pathways in the two solvents. In acetone, the solvent promotes hydrosilane activation via an outer-sphere mechanism. [21] In contrast, this pathway is not operative in chloroform, where a higher-energy yet feasible novel alternative mechanism based on metal–ligand cooperation becomes active. In this case, the pentamethylcyclopentadienyl ligand plays a key role in facilitating hydrosilane activation.

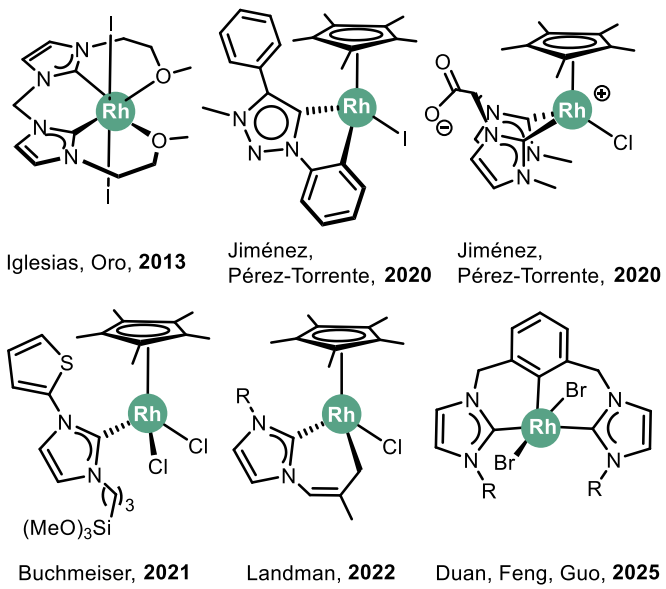


**Chart 1.** Selected NHC-Rh(III) catalysts for the hydrosilylation of alkynes.

## 2. Results and discussion

### 2.1. Alkyne hydrosilylation catalyzed by $[Cp^*RhI\{(MeIm)_2CH_2\}]^+$: Searching for the active species

The performance of $[Cp^*RhI\{(MeIm)_2CH_2\}]PF_6$ (**1**) as hydrosilylation catalyst has been investigated using the hydrosilylation of phenylacetylene with $HSiMe_2Ph$ as the model reaction. The catalytic reactions were performed under an argon atmosphere in $CDCl_3$ or acetone-$d_6$ (0.5 mL) at 298 K with 1 mol% catalyst loading, [**1**] = 1.54 mM, and monitored by $^1$H NMR with anisole as internal standard. Compound **1** showed no activity in $CDCl_3$, but a first catalytic test in acetone-$d_6$ gave a 27 % conversion of phenylacetylene in 3 h at 60 °C with complete selectivity to the β-(*Z*)-vinylsilane isomer. However, the activity data were poorly reproducible and variable conversions, typically 10–15 % in 12 h at room temperature, were achieved using catalyst samples from different preparations, although always with β-(*Z*) selectivity > 99 %. Surprisingly, a recrystallized sample of **1** in acetone/diethyl ether showed no catalytic activity at all, suggesting that the species responsible for the catalytic activity is a minor species present in the precatalyst sample. The observed constant β-(*Z*) selectivity, which is always > 99 %, suggests that the lack of reproducibility of the activity data is probably

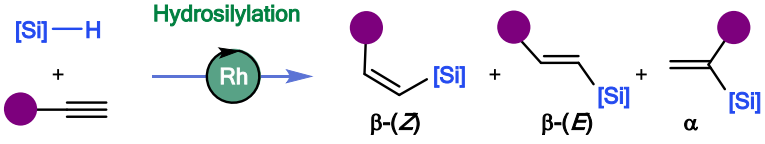


**Scheme 1.** Possible vinylsilane products in the hydrosilylation of terminal alkynes.

related to the concentration of this species in the different precatalyst samples.

Compound [Cp*RhI{(MeIm)$_2$CH$_2$}]PF$_6$ (**1**) was synthesized by reaction of the solvato species [Cp*Rh(CH$_3$CN)$_3$]$^{2+}$, prepared in situ by reaction of [Cp*RhCl$_2$]$_2$ with AgPF$_6$ in acetonitrile, with the bis-imidazolium salt [(MeImH)$_2$CH$_2$]I$_2$ in the presence of NEt$_3$ (Scheme 2). [23] The $^1$H NMR of crude **1** in acetone-$d_6$ and that of a recrystallized sample are virtually identical except for the presence of traces of the by-product [HNEt$_3$]PF$_6$ and a small residual Cp* resonance at δ 1.92 ppm. However, no catalytic activity was observed when the hydrosilylation of phenylacetylene in acetone-$d_6$ was carried out in the presence of varying amounts of [HNEt$_3$]PF$_6$ using a recrystallized sample of **1**. Similarly, recrystallized **1** was not activated in the presence of different co-catalysts, such as NaF, KI or [NH$_4$]PF$_6$ (in a 1:1 ratio), or in the presence of water (10 μl).

The excellent selectivity observed in the catalytic tests mentioned above prompted us to investigate the nature of the unknown species responsible for the catalytic activity. We hypothesized that the inertness of the Rh-I bond, which may prevent the formation of the necessary coordination vacancy, may explain the lack of activity of compound **1**. On the other hand, the synthetic method used to prepare **1** suggests that the active species may still have a labile acetonitrile ligand. For this reason, compound [Cp*Rh(NCCH$_3$){(MeIm)$_2$CH$_2$}](PF$_6$)$_2$ (**2**) was prepared by reaction of **1** with AgPF$_6$ in acetonitrile and isolated as a yellow microcrystalline solid in good yield after recrystallisation from acetonitrile/diethyl ether (Scheme 3). However, compound **2** also showed no catalytic activity in the hydrosilylation of phenylacetylene.

### 2.2. Identification of the active species

The formation of bis-NHC complexes from bis-imidazolium salts is usually a stepwise process through mono-NHC intermediates. However, only a few imidazol-2-ylidene/imidazolium species have been identified by NMR spectroscopy and/or structurally characterized. [24] Therefore, we speculated that traces of [Cp*RhI$_2${(MeIm)CH$_2$(MeImH)}]$^+$, with a coordinated NHC ligand and a dangling imidazolium cation, might account for the observed catalytic activity of **1**. The synthesis of this species was attempted by reacting [Cp*RhI$_2$]$_2$ with the bis-imidazolium salt [(MeImH)$_2$CH$_2$]I$_2$ (1:2) in methanol at room temperature, adjusting the amount of NEt$_3$ (1 equiv). However, monitoring of the reaction by $^1$H NMR showed the direct formation of the bis-NHC compound [Cp*RhI{(MeIm)$_2$CH$_2$}]I, [25] but not the expected intermediate. This result suggests that the deprotonation of the imidazolium fragment in methanol is very fast. Interestingly, when the reaction was performed in acetonitrile under the same conditions, a new set of resonances attributed to an intermediate species was observed after 2 h. This species, which was isolated as dark red crystals by layering a dichloromethane solution of the reaction crude with pentane, was characterized as the ion-pair compound [Cp*RhI$_2${(MeIm)CH$_2$(MeImH)}][Cp*RhI$_3$] (**3**).

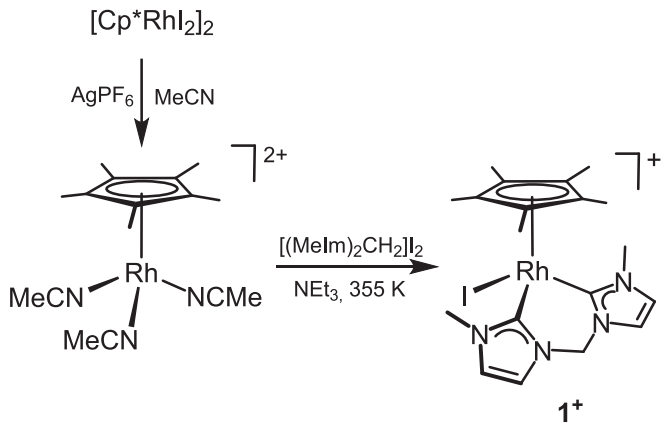


**Scheme 2.** Synthesis of [Cp*RhI{(MeIm)$_2$CH$_2$}]PF$_6$ (**1**).

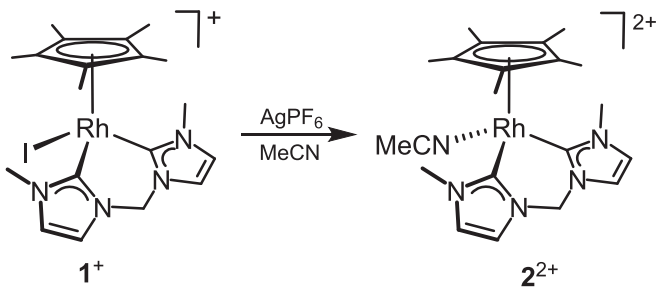


**Scheme 3.** Synthesis of [Cp*Rh(NCCH$_3$){(MeIm)$_2$CH$_2$}](PF$_6$)$_2$ (**2**).

The crystal structure of **3** contains the cation [Cp*RhI$_2${(MeIm)CH$_2$(MeImH)}]$^+$ and the anion [Cp*RhI$_3$]$^-$, both exhibiting a semi-sandwich structure, in which each η$^5$-Cp* ligand formally occupies three coordination sites [Ct1-Rh1 1.832(8), Ct2-Rh2 1.785(8) Å, Fig. 1]. The coordination sphere of the metal centers is completed by three iodido ligands in [Cp*RhI$_3$]$^-$ (Rh-I 2.721 Å, av.) and by two iodido ligands (Rh-I 2.724 Å, av.) and the κ*C*-NHC moiety of [(MeIm)CH$_2$(MeImH)]$^+$ [C1-Rh1 2.052(6) Å]. Notably, short intermolecular contacts CH···I were observed between the cation [Cp*RhI$_2${(MeIm)CH$_2$(MeImH)}]$^+$ and the anion [Cp*RhI$_3$]$^-$, namely C9-H9···I4 and C7-H7A···I4 (Fig. 1). As for the coordination of the NHC ligand to Rh1, an almost ideal arrangement of the C1-N2-C3-C4-N5 ring with respect to the Rh1-C1 bond was observed (pitch angle, ϑ 8.2°, yaw angle, ψ 0.4°).

To the best of our knowledge, even though the related anion [Cp*RhCl$_3$]$^-$ has been already structurally characterized, [26] this is the first time the crystal structure of the iodo derivative [Cp*RhI$_3$]$^-$ is reported. Also, it is worth mentioning that the crystal structure of the cation [Cp*RhI$_2${(MeIm)CH$_2$(MeImH)}]$^+$ is similar to that described for the related NHC derivatives [Cp*RhCl$_2${(RIm')CH$_2$(RIm'H}]$^+$. [27]

Using the appropriate stoichiometric ratio of [Cp*RhI$_2$]$_2$, [(MeImH)$_2$CH$_2$]I$_2$ and NEt$_3$ (1:1:1) in acetonitrile it was possible to

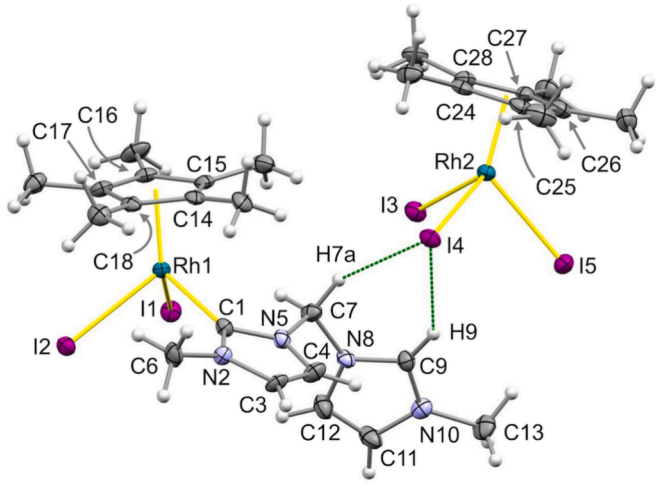


**Fig. 1.** ORTEP view of [Cp*RhI$_2${(MeIm)CH$_2$(MeImH)}][Cp*RhI$_3$] in **3**. Thermal ellipsoids are at 50 % probability. Selected bond lengths (Å) and angles (°) are: Ct1-Rh1 1.832(8), Ct2-Rh2 1.785(8), C(1)-Rh(1) 2.052(6), Rh(1)-I(1) 2.7213(6), Rh(1)-I(2) 2.7270(6), Rh(2)-I(3) 2.7213(7), Rh(2)-I(4) 2.7347(6), Rh(2)-I(5) 2.7074(7), C(1)-Rh(1)-I(1) 95.88(17), C(1)-Rh(1)-I(2) 95.57(16), I(1)-Rh(1)-I(2) 87.673(18), I(5)-Rh(2)-I(4) 91.924(19), I(3)-Rh(2)-I(4) 96.112(19), I(5)-Rh(2)-I(3) 88.90(2), Ct1-Rh1-I1 123.2(2), Ct1-Rh1-I2 121.4(2), Ct1-Rh1-C1 124.2(3), Ct2-Rh2-I3 123.1(2), Ct2-Rh2-I4 122.3(2), Ct2-Rh1-I5 125.5(2), C9-H9···I4: C9-H9 0.90(6), H9-I4 3.14(7), C9-I4 3.906(7), C9-H9-I4 143(5); C7-H7A···I4: C7-H7A 1.05(6), H7A-I4 2.74(6), C7-I4 3.688(7), C7-H7A-I4 151(4). Ct1, centroid of C14, C15, C16, C17, and C18; Ct2, centroid of C23, C24, C25, C26, and C27.

prepare compound **3** as a microcrystalline dark red solid in 92 % yield (Scheme 4). The spectroscopic data in solution are in agreement with the ion-pair structure found in the solid state. In fact, both ions were observed in the HRMS in acetonitrile. The $^1$H NMR spectrum in $CDCl_3$ showed a singlet resonance at δ 10.20 ppm corresponding to the NCHN of the imidazolium fragment, and two singlets at δ 1.91 and 2.06 ppm corresponding to the Cp* ligands of the cation and the anion, respectively. In addition, consistent with the unsymmetrical structure of the cation, the =CH protons of the NHC and the imidazolium fragments were observed as four resonances between δ 8.10–7.00 ppm. Finally, the diastereotopic protons of the > $CH_2$ fragment were observed as a broad AB system at δ 7.49 ppm.

Compound **3** has been shown to be a very efficient hydrosilylation catalyst. In fact, under standard conditions described above, the hydrosilylation of phenylacetylene with $HSiMe_2Ph$ in acetone-$d_6$ gave full conversion to the β-(*Z*)-vinylsilane product (> 99 %) in 5 min. Therefore, it can be inferred that the species responsible for the catalytic activity of non-recrystallized samples of **1** is most likely $[Cp^*RhI_2\{(MeIm)CH_2(MeImH)\}]^+$, the cation of compound **3**. Indeed, in the $^1$H NMR spectrum of **3** in acetone-$d_6$, the Cp* resonance of the cation was observed at δ 1.92 ppm. This chemical shift is identical to that of the residual Cp* resonance observed in the NMR spectrum of **1** in the same solvent.

### 2.3. Redesign of the catalyst

The excellent hydrosilylation catalytic activity of the ion-pair compound **3** strongly suggests a catalyst redesign. Predictably, neither the anion $[Cp^*RhI_3]^-$ nor the imidazolium fragment in the cationic $[Cp^*RhI_2\{(MeIm)CH_2(MeImH)\}]^+$ species should play a significant role in the hydrosilylation reaction. In fact, the 1,3-dimethylimidazolium iodide salt, [IMeH]I, does not catalyze the hydrosilylation of phenylacetylene. Therefore, $[Cp^*RhI_2(IMe)]$ (IMe = 1,3-dimethylimidozol-2-ylidene) could be considered as a simplified version of the catalytic active species.

Compound $[Cp^*RhI_2(IMe)]$ (**4**) was prepared according to a well-established procedure reported in the literature for related chloro complexes. [28] This two-step procedure entails the formation of the Ag-IMe species, prepared by reaction of the imidazolium salt [IMeH]I with $Ag_2O$ in dichloromethane, followed by reaction with $[Cp^*RhI_2]_2$. However, following this procedure, compound **4** was obtained impurified with the bis-NHC cationic species $[Cp^*RhI(IMe)_2]I$. [29] As a result, purification by chromatography (silica gel, dichloromethane/methanol 1:1) is required thereby resulting in very low yields of **4** (< 30 %).

The formation of $[Cp^*RhI(IMe)_2]I$ in the synthesis of **4** suggests the lability of the iodide ligands. Accordingly, we attempted the synthesis of **4** from $[Cp^*RhCl_2]_2$ via the intermediate $[Cp^*RhCl_2(IMe)]$, followed by anion metathesis with NaI. Using this approach, compound **4** was obtained in a single step with 81 % yield (Scheme 5).

The $^1$H NMR spectrum of **4** in $CDCl_3$ showed three resonances at *δ* 7.02 (=CH), 4.04 ($NCH_3$) and 1.90 (Cp*), in agreement with the expected $C_s$ symmetry. The formation of the Rh−NHC bond was confirmed by the absence of the characteristic low-field $^1$H signal of the H2 proton of the imidazolium salt precursor and the presence of a $^{13}$C doublet at *δ* 166.7 ppm ($J_{C\text{-}Rh}$ = 47.4) which was assigned to the carbenic carbon

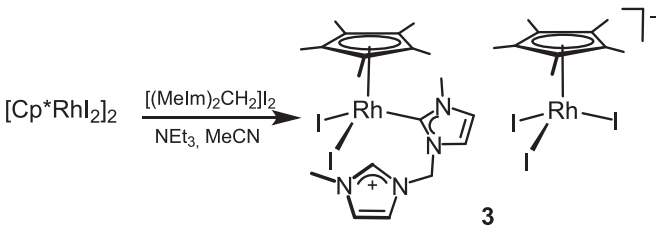


**Scheme 4.** Synthesis of $[Cp^*RhI_2\{(MeIm)CH_2(MeImH)\}][Cp^*RhI_3]$ (**3**).

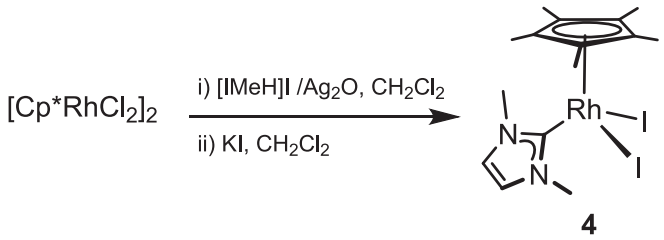


**Scheme 5.** Synthesis of $[Cp^*RhI_2(IMe)]$ (**4**).

atom. Recrystallization from dichloromethane/pentane afforded the compound as dark red microcrystals suitable for X-ray diffraction.

The crystal structure of **4** shows a rhodium(III) center with a slightly distorted three-legged piano-stool geometry as a consequence of the $\eta^5$-coordination of the Cp* ligand [Ct-Rh 1.838(6) Å]. The IMe and two iodido ligands complete the coordination sphere of the rhodium center [I1-Rh 2.7184(7), I2-Rh 2.7260(8), C1-Rh 2.058(8) Å]. Similar to **3**, an almost ideal arrangement of the C1-N2-C3-C4-N5 ring of the NHC ligand with respect to the Rh-C1 bond is observed (pitch angle, ϑ 8.0°, yaw angle, ψ 0.4°). It is worth mention that, despite the fact that related $[(\eta^5\text{-}C_5Me_4R)RhCl_2(R_2Im)]$ derivatives have been structurally characterized, [28b] to the best of our knowledge, **4** is the first iodo derivative whose structure has been determined, so far (Fig. 2).

Compound **4** efficiently catalyzed the hydrosilylation of phenylacetylene with $HSiMe_2Ph$ in acetone-$d_6$ with 99 % conversion in less than 5 min, and complete selectivity to the β-(*Z*)-vinylsilane product. Interestingly, compound **4** also showed good catalytic activity in $CDCl_3$, although significantly lower than in acetone-$d_6$. Under the same conditions, 43 % conversion to the β-(*Z*)-vinylsilane product was achieved in 5 min, reaching full conversion, >99 %, in 55 min.

The lability of the iodido ligands in **4** prompted the synthesis of related cationic solvated species. The bis-acetonitrile compound $[Cp^*Rh(NCCH_3)_2(IMe)][BF_4]_2$ (**5**) was obtained by reacting **4** with two equivalents of $AgBF_4$ in acetonitrile, and isolated as a yellow solid in 78 % yield (Scheme 6). The acetonitrile ligands in **5** were observed at δ 2.14 ppm and 0.4 ppm in the $^1$H and $^{13}C\{^1H\}$ NMR spectra in $CD_3CN$, respectively, suggesting slow exchange with the deuterated acetonitrile solvent. As expected, reaction of **4** with one equiv of $AgBF_4$ in

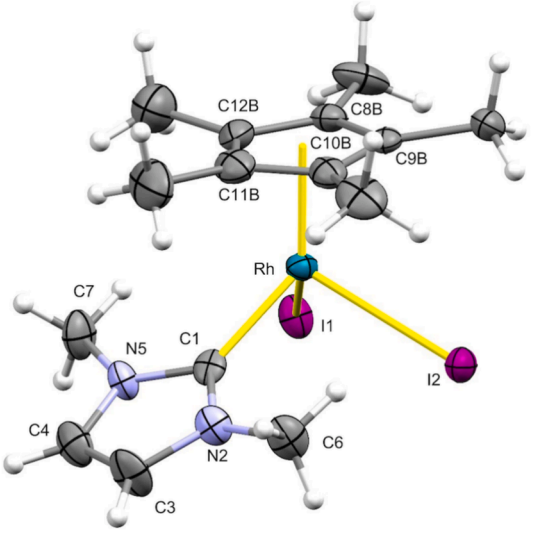


**Fig. 2.** ORTEP view of $[Cp^*RhI_2(IMe)]$ (**4**). Thermal ellipsoids are at 50 % probability. Only one component of the positionally disordered Cp* ligand is shown for clarity. Selected bond lengths (Å) and angles (°) are: I1-Rh 2.7184(7), I2-Rh 2.7260(8), C1-Rh 2.058(8), Ct-Rh 1.838(6), Ct-Rh-C1 126.77(20), Ct-Rh-I1 123.53(8), Ct-Rh-I2 118.17(8), I1-Rh-I2 87.33(2), C1-Rh-I1 92.56(18), C1-Rh-I2 99.24(20). Ct, centroid of C8B, C9B, C10B, C11B, and C12B.

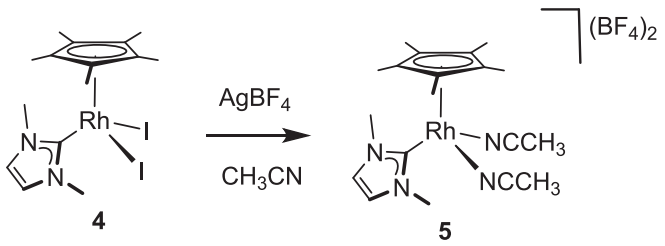


**Scheme 6.** Synthesis of $[Cp^*Rh(NCCH_3)_2(IMe)][BF_4]_2$ (**5**).

acetonitrile resulted a mixture containing the solvate compound $[Cp^*Rh(NCCH_3)I(IMe)][BF_4]$ along with **4** and **5**.

Similar to **4**, the rhodium(III) center of **5** exhibits a slightly distorted three-legged piano-stool geometry with $\eta^5$-coordination of the Cp* ligand [Ct-Rh 1.808(6) Å, N18-Rh-N21 83.38(18), C1-Rh-N21 88.92 (19), C1-Rh-N18 92.7(2)] (Fig. 3). The IMe and two acetonitrile ligands complete the coordination sphere of the rhodium center [Rh-C1 2.075 (6), Rh-N21 2.091(4), Rh-N18 2.105(5) Å]. Also, an almost ideal arrangement of the C1-N2-C3-C4-N5 ring of the NHC ligand with respect to the Rh-C1 bond is observed (pitch angle, ϑ 0.9°; yaw angle, ψ 2.3°).

Compound **5** has also been shown to be an active catalyst for hydrosilylation of phenylacetylene with $HSiMe_2Ph$, exhibiting complete selectivity to the β-(*Z*)-vinylsilane product. Catalyst **5** is less active than **4** in acetone-$d_6$, affording 87 % conversion in 30 min. Notably, the catalytic activity of **5** in $CDCl_3$ is slightly higher than that of **4**, achieving 96 % conversion in just 20 min.

### 2.4. Hydrosilylation of 1-alkynes catalyzed by 4: Substrate scope

The performance of catalyst **4** in the hydrosilylation of a series of terminal alkynes in acetone-$d_6$ at room temperature was explored using a catalyst loading of 1 mol% and $HSiMe_2Ph$ as hydrosilane. As shown in Chart 2, compound **4** was found to be effective in the selective formation of β-(*Z*)-vinylsilanes from aryl- or alkyl-substituted terminal alkynes with excellent conversions in short reaction times.

The hydrosilylation of ring-substituted phenylacetylene derivatives proceeded efficiently to selectively afford the corresponding β-(*Z*)-vinylsilane derivatives quantitatively. The catalytic activity increased slightly (with respect to phenylacetylene) with an electron-donating group in the para position (−Me or −OMe) while decreased slightly with an electron-withdrawing substituent ($-CF_3$). The hydrosilylation of *meta*- and *ortho*-substituted phenylacetylene derivatives required slightly longer reaction times, especially the hydrosilylation of 1-chloro-2-ethynylbenzene which required 270 min to achieve 85 % conversion. The hydrosilylation of the bulky 2-ethynyl-1,3,5-trimethylbenzene was only somewhat slower than that of 1-ethynyl-2-methylbenzene, giving 97 % conversion to the β-(*Z*)-vinylsilane product in 90 min. Cyclohexylacetylene was quantitatively transformed in the β-(*Z*)-vinylsilane derivative in 30 min, whereas 1-ethynylcyclohex-1-ene required 5 h.

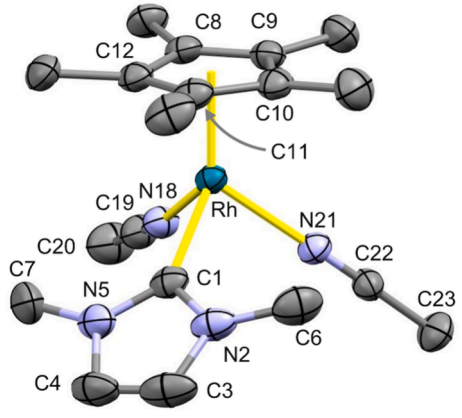


**Fig. 3.** ORTEP view of $[Cp^*Rh(NCCH_3)_2(IMe)]^{2+}$ in $[Cp^*Rh(NCCH_3)_2(IMe)][BF_4]_2$ (**5**). Thermal ellipsoids are at 30 % probability. Selected bond lengths (Å) and angles (°) are: Rh-C1 2.075(6), Rh-N21 2.091(4), Rh-N18 2.105(5), Rh-Ct 1.808(6), N18-Rh-N21 83.38(18), C1-Rh-N21 88.92(19), C1-Rh-N18 92.7 (2), Ct-Rh-C1 128.4(2), Ct-Rh-N21 126.3(2), Ct-Rh-N18 124.1(2). Ct, centroid of C8, C9, C10, C11, and C12.

The hydrosilylation of a linear aliphatic 1-alkyne, such as 1-octyne, was complete in only 2 min with full selectivity to the β-(*Z*)-vinylsilane derivative. As expected, the hydrosilylation of the bulky prop-2-yn-1-ylbenzene was much slower reaching, 95 % conversion to the β-(*Z*)-vinylsilane product in 80 min. In contrast, the hydrosilylation of a branched aliphatic alkyne, such as the bulky 3,3-dimethyl-1-butyne, was much slower and unselective, yielding a mixture of vinylsilane isomers and 3,3-dimethylbut-1-ene, one of the dehydrogenative silylation products after 12 h. Similarly, the hydrosilylation of trimetylsilylacetylene was unselective (Table 1).

The hydrosilylation of functionalized aliphatic 1-alkynes such as but-3-yn-1-ol, or methyl propargyl ether was completely selective towards the β-(*Z*)-vinylsilane derivatives (Chart 2). However, the hydrosilylation of phenyl propargyl sulfide was unselective with a 62 % conversion in 12 h (Table 1). In contrast, no conversion was observed after 60 min in the hydrosilylation of 2-ethynylpyridine or *N*,*N*-dimethylbut-3-yn-1-amine, probably due to the catalyst deactivation by coordination of the *N*-donor function of the substrates. Finally, the hydrosilylation of aliphatic and aromatic diynes, such as octa-1,7-diyne, 1,3-diethynylbenzene and 1,4-diethynylbenzene, selectively gave the corresponding β-(*Z*)-β-(*Z*)-divinylsilane derivatives in 50–90 min (Chart 2).

Compound **4** also catalyzed the hydrosilylation of both symmetric (3-hexyne) and asymmetric (1-phenyl-1-propyne) internal alkynes under the same conditions. In acetone-$d_6$, the hydrosilylation of 3-hexyne with $HSiMe_2Ph$ proceeds slowly at room temperature, selectively affording the *syn*-addition (*E*) product and reaching full conversion after 12 h. 1-Phenyl-1-propyne reacted more slowly, reaching 98 % conversion after 18 h, yielding a mixture of the two possible *syn*-addition products, *syn*-(*E*) and *syn*-(*Z*), in a 76:24 ratio, respectively (see the Supporting Information).

As can be observed in the reaction profile for the hydrosilylation of 1,3-diethynylbenzene with $HSiMe_2Ph$ (1:2 ratio) in acetone-$d_6$, the hydrosilylation of the first ethynyl group is faster than that of the second one. The maximum concentration of the β-(*Z*)-vinylsilane-alkynyl intermediate in the reaction mixture reaches 50 % after 11 min, after which it decreases steadily as it transforms into the β-(*Z*)-β-(*Z*)-divinylsilane derivative (Fig. 4).

The performance of catalyst **4** in the hydrosilylation of phenylacetylene was evaluated using different hydrosilanes. As expected, the hydrosilylation with the bulkiest hydrosilanes $HSiMePh_2$ and $HSiPh_3$ was slower, especially with the latter. However, it proceeded with complete selectivity to the β-(*Z*)-vinylsilane product. Interestingly, a 70 % hydrosilane conversion to the β-(*Z*)-vinylsilane product was achieved with $HSiEt_3$ in 2 h. Finally, the hydrosilylation with the bulky $HSiMe(OSiMe_3)_2$ was also slow, with a selectivity of 94 % for the β-(*Z*)-vinylsilane product and 6 % for the β-(*E*)-vinylsilane isomer (Chart 3). On the other hand, the hydrosilylation of phenylacetylene with the reactive hydrosilane $H_2SiPh_2$ (2:1) catalyzed by **4** in $CDCl_3$ at room temperature is unselective, yielding a mixture of mono- and di-alkenylsilanes with complete β-regioselectivity but no *Z*-stereocontrol (see the Supporting Information).

The hydrosilylation of phenylacetylene with $HSiMe_2Ph$ catalyzed by **4** proceeds efficiently in acetone-$d_6$ to afford the β-(*Z*)-vinylsilane product with 99 % conversion in less than 5 min. Under the same conditions, in the absence of phenylacetylene, hydrosilylation of acetone-$d_6$ took place with 40 % conversion of hydrosilane in 4 h. The $^1H$ NMR of the reaction mixture showed a singlet resonance at δ 0.40 ppm for the hydrosilylation reaction product, $PhMe_2Si\text{-}O\text{-}CH(CD_3)_2$, and a smaller resonance at δ 0.34 ppm corresponding to $PhMe_2Si\text{-}OH$, the hydrolysis

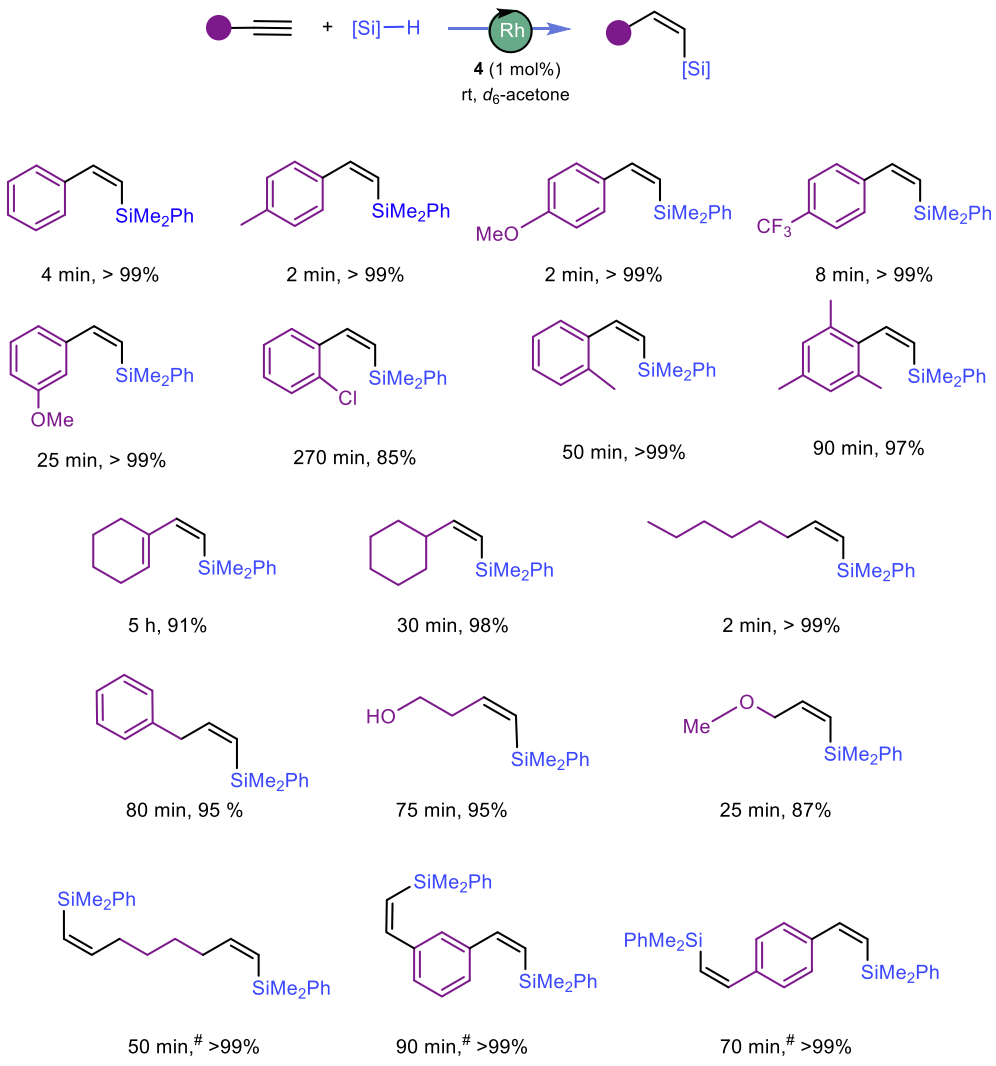


**Chart 2.** Scope of the hydrosilylation of terminal alkynes with $HSiMe_2Ph$ catalyzed by $[Cp^*RhI_2(IMe)]$ (**4**). Reactions were carried out in acetone-$d_6$ at 298 K using a $HSiMe_2Ph$/RC≡CH/**4** ratio of 100/100/1, [**4**] = 2.75 mM. # $HSiMe_2Ph$/RC≡CH/**4** ratio of 200/100/1. Conversion and selectivities determined by $^1H$ NMR spectroscopy using anisole as internal standard.

**Table 1**
Hydrosilylation of terminal alkynes with $HSiMe_2Ph$ catalyzed by $[Cp^*RhI_2(IMe)]$ (**4**).[a,b.]

| entry | alkyne | time (h) | conv. (%) | β-(*Z*) (%) | β-(*E*) (%) | α (%) | alkene (%) |
|---|---|---|---|---|---|---|---|
| 1 | 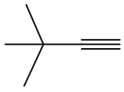 | 12 | >99 | 24 | 48 | 5 | 23 |
| 2 | 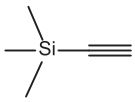 | 12 | >99 | – | 33 | 62 | 5 |
| 3 | 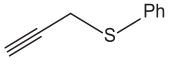 | 12 | 62 | 43 | 5 | 14 | – |

a) Reactions were carried out in acetone-$d_6$ at 298 K using a $HSiMe_2Ph$/RC≡CH/**4** ratio of 100/100/1, [**4**] = 2.20 mM. b) Conversion and selectivities determined by $^1H$ NMR spectroscopy using anisole as internal standard.

product of the hydrosilane (see the Supporting Information). In general, the hydrosilylation of acetone was not observed in the alkyne hydrosilylation experiments, except for bulky branched aliphatic alkynes or phenyl propargyl, where trace amounts formed after the extended reaction time required (Table 1). As can be observed in the reaction profile for the hydrosilylation of cyclohexylacetylene with $HSiMePh_2$ in a 1:2 ratio, the hydrosilylation of cyclohexylacetylene is much faster than that of the acetone-$d_6$ (Fig. 5).

Catalyst $[Cp^*RhI_2(IMe)]$ (**4**) has shown excellent stability with the activity being maintained in successive additions of reactants. The

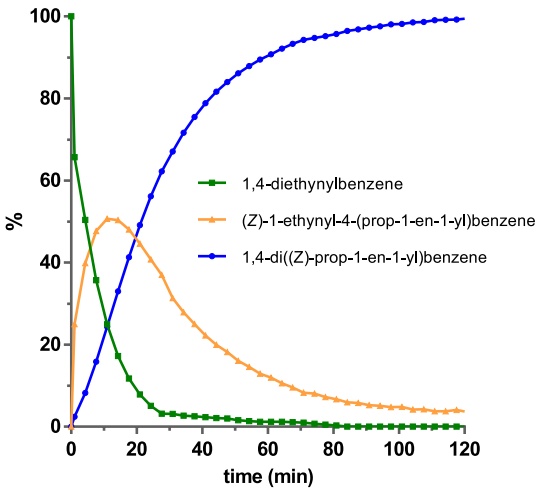


**Fig. 4.** Reaction profile for the hydrosilylation of 1,3-diethynylbenzene with $HSiMe_2Ph$ (1:2) catalyzed by **4** (1 mol%) in acetone-$d_6$ (0.4 mL) at 298 K.

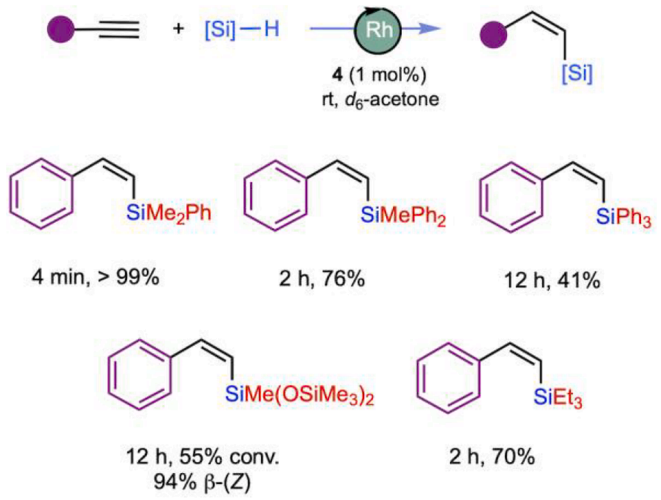


**Chart 3.** Scope of the hydrosilylation of phenylacetylene with different hydrosilanes ($HSiR_3$) catalyzed by [Cp*$RhI_2$(IMe)] (**4**). Reactions were carried out in acetone-$d_6$ (0.4 mL) at 298 K using a $HSiR_3$/PhC≡CH/**4** ratio of 100/100/1, [**4**] = 2.75 mM. Conversion and selectivities determined by $^1$H NMR spectroscopy using anisole as internal standard.

hydrosilylation of phenylacetylene with $HSiMe_2Ph$ catalysed by **4** (1 mol %) proceeded to full conversion in less than 5 min at room temperature. Adding new reactants (phenylacetylene and $HSiMe_2Ph$) after the reaction completion resulted in the consumption of the reactants. Monitoring of the reaction by $^1$H NMR spectroscopy showed that, after eight consecutive experiments, the only product obtained was the β-(*Z*)-vinylsilane isomer (see the Supporting Information). Thus, the catalyst precursor was able to perform at least eight consecutive catalytic cycles (TON = 800) without losing activity or selectivity towards the β–(*Z*)-vinylsilane product. Additionally, the hydrosilylation can be performed on a preparative scale retaining high conversions and complete β-(*Z*) selectivity, as demonstrated by the synthesis of dimethyl(phenyl)(*Z*-styryl)silane (see the Experimental section).

The influence of the catalyst loading in the hydrosilylation of phenylacetylene with $HSiMe_2Ph$ was also studied. A series of experiments were carried out in which the catalyst loading was reduced from 1 to 0.025 mol% (Fig. 6). Using a catalyst load as low as 0.025 mol% (250 ppm), 85 % hydrosilane conversion to the β-(*Z*)-vinylsilane product was achieved in only 5 h, with a $TOF_{50}$ of 1500 $h^{-1}$. However, the highest

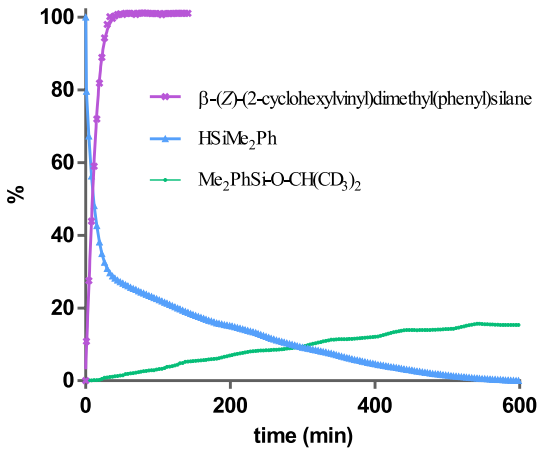


**Fig. 5.** Reaction profile for the competitive hydrosilylation of cyclohexylacetylene and acetone-$d_6$ with $HSiMe_2Ph$ (1:2) catalyzed by **4** (1 mol%) in acetone-$d_6$ (0.4 mL) at 298 K.

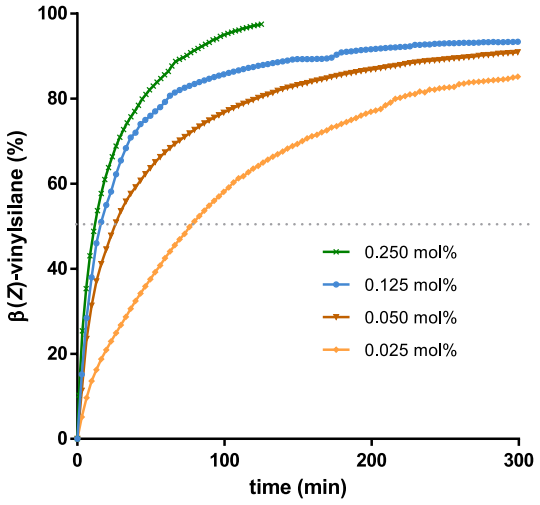


**Fig. 6.** Reaction profile of conversion *vs* time for the hydrosilylation of phenylacetylene with $HSiMe_2Ph$ (1:1) catalyzed by **4** in acetone-$d_6$ (0.4 mL) at 298 K at different catalyst loadings.

activity was obtained using 0.05 mol% (500 ppm) with a $TOF_{50}$ = 2300 $h^{-1}$. Notably, the attained average TOFs of 620 and 360 $h^{-1}$ are higher than those reported for the hydrosilylation of phenylacetylene by cationic Rh(I) complexes bearing picolyl-functionalized NHC ligands [12b] (see the Supporting Information).

### 2.5. *Mechanistic studies on the hydrosilylation of 1-alkynes catalyzed by **4***

To gain detailed insight into the reaction mechanism of β-(*Z*)-selective alkyne hydrosilylation catalyzed by complex **4**, we carried out a DFT computational study using the hydrosilylation of phenylacetylene with $HSiMe_2Ph$ as model reaction (see Computational Details for methodological information).

Given the very good activities reported in acetone under mild conditions, we envisaged a non-classical reaction mechanism in which the hydrosilane is activated in an heterolytic manner by assistance of solvent acetone molecules. [21] Notably, complex **4** contains two iodide ligands, which have been experimentally shown to be labile. Since the substitution of an anionic ligand by neutral substrates (alkyne, hydrosilane or acetone) would introduce considerable error in gas-phase calculations with implicit solvent corrections, we initially replaced a iodido

ligand by $HSiMe_2Ph$. This process has a Gibbs free energy cost of 8.4 kcal·mol$^{-1}$ and is entropically favored, given the much lower concentration of the catalyst relative to the reactants. These results suggest that, once the iodide ligand dissociates, it is unlikely to re-coordinate to the metal center. The resulting complex, considered the catalytically active species in our study, is designated as species **A**. The proposed catalytic cycle is provided in Fig. 7.

The $\eta^1$-H(Si) coordination of the hydrosilane in **A** increases the electrophilicity of the silicon atom, thereby facilitating the interaction of an acetone molecule at the backside of the hydrosilane. This affords species **B**, which is 4.2 kcal·mol$^{-1}$ more stable in Gibbs energy. Subsequently, the silyl group of the hydrosilane is transferred to the oxygen atom of acetone, leading to the heterolytic cleavage of the H–Si bond. This process occurs via $\mathbf{TS_{BC}}$, which has a relative Gibbs energy of 4.0 kcal·mol$^{-1}$, corresponding to an energy barrier of 8.2 kcal·mol$^{-1}$. As a result, a neutral hydrido complex is formed together with a oxocarbenium ion, corresponding to a cationic silylated acetone species. To avoid splitting the system into two fragments with different charges—which, as previously noted, could introduce errors associated with long-range Coulomb interactions—both fragments were included in the same calculation. The resulting species, **C**, has a relative Gibbs energy of –3.2 kcal·mol$^{-1}$, making it 1.0 kcal·mol$^{-1}$ more stable than **B**. Species **C** is further stabilized through interaction with a phenylacetylene molecule, forming intermediate **D** with a relative Gibbs energy of –12.3 kcal·mol$^{-1}$. The silyl group is then transferred from acetone to the β-carbon of phenylacetylene via $\mathbf{TS_{DE}}$. This step presents a Gibbs energy barrier of 15.7 kcal·mol$^{-1}$ (the Gibbs energy difference between $\mathbf{TS_{DE}}$ and **D**) and yields a carbocationic species bearing a newly formed C–Si bond, denoted as **E**, with a relative Gibbs energy of –1.8 kcal·mol$^{-1}$.

In the final step, the hydride ligand bound to the Rh atom is transferred to the α-carbon atom of the silylated carbocation, regenerating the active species **A**. This transformation determines the reaction selectivity, leading to either the β-(*Z*)- or β-(*E*)-vinylsilane product. Notably, the transition state leading to β-(*Z*)-vinylsilane, $\mathbf{TS_{EA}}$, is 19.5 kcal·mol$^{-1}$ more stable than that leading to β-(*E*)-vinylsilane, $\mathbf{TS_{EA}}$', a difference attributed to the greater steric hindrance in the latter, which fully accounts for the exclusive formation of the β-(*Z*)-vinylsilane. [21,23].

The effective Gibbs energy barrier of this process is 15.7 kcal·mol$^{-1}$ (the Gibbs energy difference between $\mathbf{TS_{EA}}$ and **D**). Accordingly, the energy span of the catalytic cycle is also 15.7 kcal·mol$^{-1}$, governed by $\mathbf{TS_{DE}}$ and $\mathbf{TS_{EA}}$, both having a relative Gibbs energy of 3.4 kcal·mol$^{-1}$. This relatively low energy barrier agrees with the experimentally observed fast reaction rate at room temperature in acetone-$d_6$.

At this point, it is worth noting that the reaction—though slower—still proceeds rapidly in the absence of acetone (in $CDCl_3$). This observation suggests the operation of an alternative reaction pathway with a higher energy profile under such conditions. Experimentally, the iodido ligands in complex **4** have been found to be labile. Moreover, complex $[Cp^*Rh(IMe)(CH_3CN)_2]^{2+}$ (**5**) is also reported herein to be catalytically active in the hydrosilylation of phenylacetylene in $CDCl_3$. Consequently, this species was considered in further mechanistic investigations.

Given the lability of the acetonitrile ligands and the significantly higher concentrations of hydrosilane and alkyne under catalytic conditions, mechanistic studies were initiated with the complex analogous to **5**, in which an acetonitrile ligand had been replaced by a $HSiMe_2Ph$ ligand $\eta^1$-H(Si) coordinated to the metal center. This complex is referred to as **F** to maintain consistency with the preceding nomenclature. The proposed reaction mechanism in the absence of acetone is provided in Fig. 8.

Probably the main issue when addressing this reaction mechanism derives from hydrosilane (or alkyne) activation. In this respect, we propose a mechanism in which hydrosilane activation involves the active participation of the Cp* ligand. Although Cp* is traditionally regarded as an innocent ligand, recent studies have highlighted its potential for non-innocent behavior. [30] Interestingly, reductive coupling involving Rh − H and Rh − $C_5Me_5$ functionalities in Rh(III) complexes results in the formation of [$\eta^4$-Cp*H] species with concomitant metal reduction to Rh(I). [31] Related [$\eta^4$-Cp*H]-Ir(I) species have been proposed as intermediates in the hydrogenation of ketones through a bifunctional reaction mechanism. [32] Remarkably, reversible hydrogen migration from the metal center to the Cp* ring, which acts as a proton relay, has been observed in several stoichiometric and catalytic

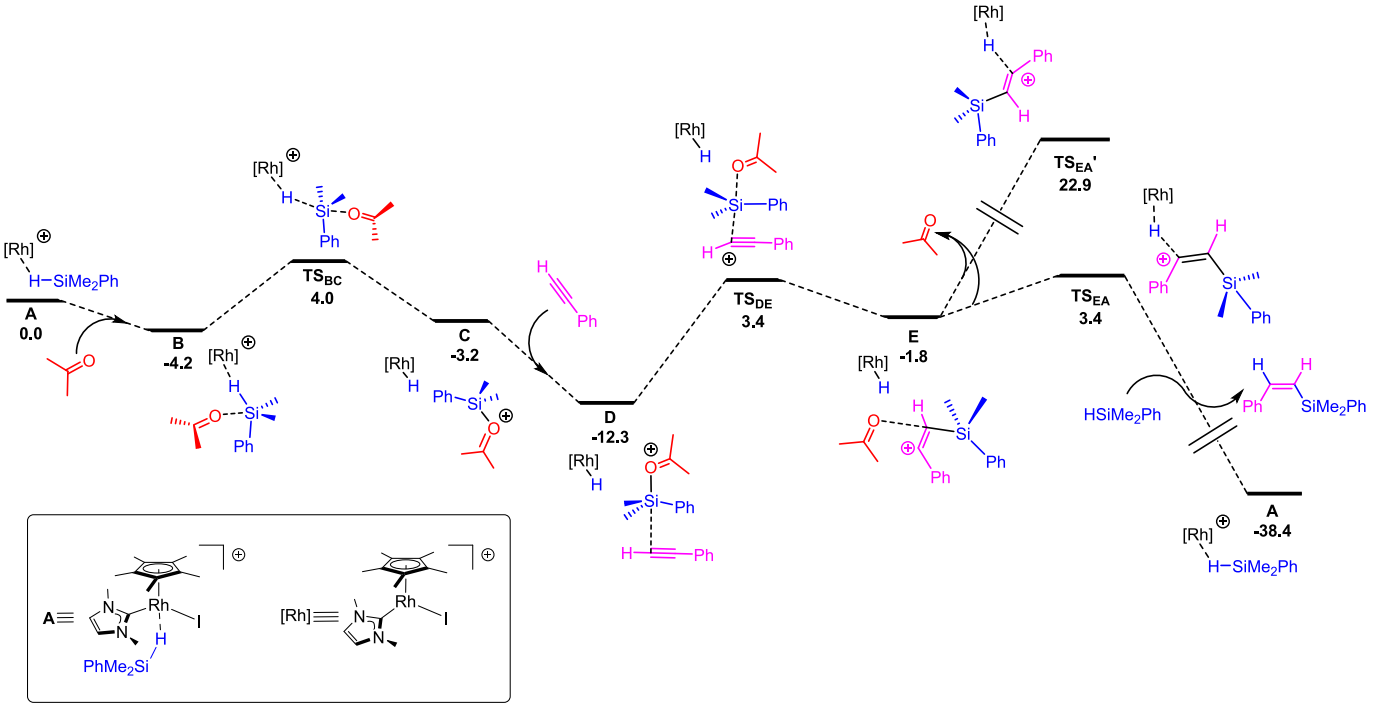


**Fig. 7.** DFT calculated Gibbs free energy profile (in kcal·mol$^{-1}$, relative to **A** and the isolated molecules) for the hydrosilylation of phenylacetylene in acetone.

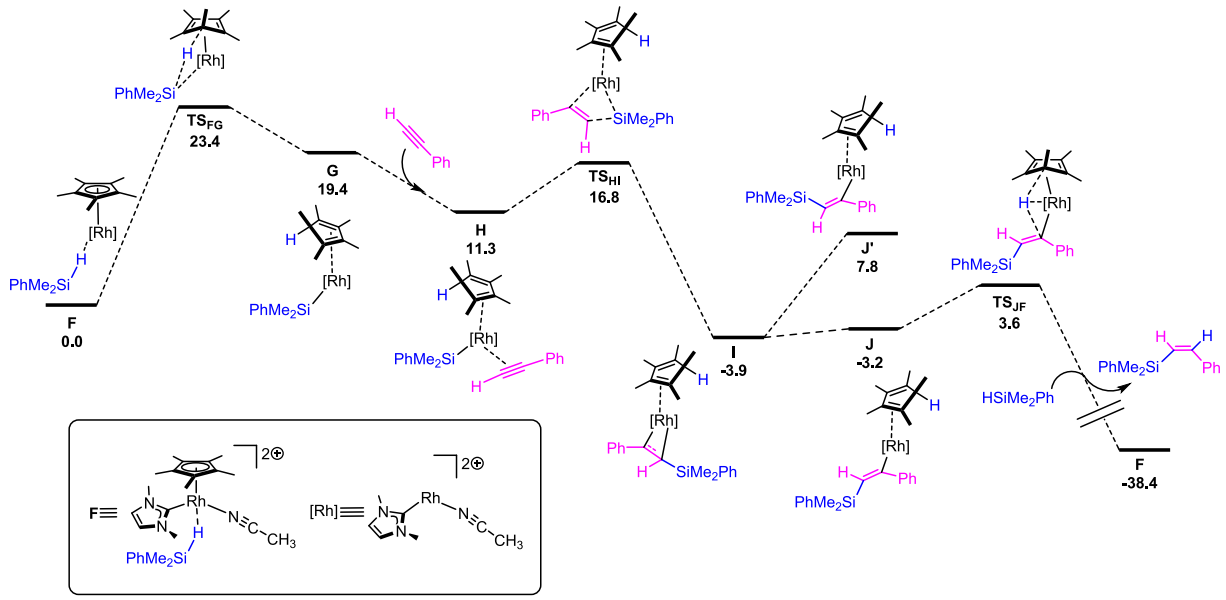


**Fig. 8.** DFT calculated Gibbs free energy profile (in kcal·mol$^{-1}$, relative to **F** and the isolated molecules) for the hydrosilylation of phenylacetylene in the absence of acetone.

reactions. [33] In addition, protonated metallocene species have been shown to behave as strong proton donors with application in proton-coupled electron transfer reactions. [34].

Based on these findings, we propose that the hydrosilane is activated through a cooperative interaction with the Cp* ligand via transition state **TS$_{FG}$** (Fig. 9a). This step results in the formation of a Rh–Si bond and protonation of the Cp* moiety, with an associated Gibbs energy barrier of 23.4 kcal·mol$^{-1}$. The reaction yields silyl intermediate **G**, which lies 19.4 kcal·mol$^{-1}$ above the reference Gibbs energy, in which the newly formed Cp*H binds to the metal center through an $\eta^4$ coordination mode.

The subsequent step involves the alkyne's C≡C bond coordination to the metal center, yielding intermediate **H**, 8.1 kcal·mol$^{-1}$ more stable than **G**. Note that, to accommodate the alkyne, the coordination mode of the Cp*H ligand switches from $\eta^4$ to $\eta^2$. We also considered the possibility of retaining the $\eta^4$ coordination mode of the Cp*H ligand in H while allowing decoordination of the acetonitrile ligand. However, this structure was higher in Gibbs free energy by 13.0 kcal·mol$^{-1}$ and was therefore discarded.

Then, the silyl fragment migrates from the metal center to the β-carbon of the alkyne, affording the metallacyclopropene (or $\eta^2$-vinylsilane) intermediate **I**. Such an intermediate has a relative Gibbs energy of –3.9 kcal·mol$^{-1}$, being 15.2 kcal·mol$^{-1}$ more stable than **H**. This reaction step proceeds via **TS$_{HI}$**, with a relative Gibbs energy of 16.8 kcal·mol$^{-1}$. The opening of the metallacyle in **I** might lead to two different silylvinylene isomers, **J** and **J'**, which would evolve, respectively, to β-(*Z*)- and β-(*E*)-vinylsilane products. Notably, the **J** isomer lies 11.0 kcal·mol$^{-1}$ lower in Gibbs energy, evidencing a complete preference for the β-(*Z*)-vinylsilane product, in agreement with the experimental findings. In general terms, we attribute such a Gibbs energy difference to lower steric hindrance in **J**, in line with our previous studies in the β-(*Z*)-hydrosililation of alkynes by Rh(III)–triazolylidene catalysts. [22].

Finally, the β-(*Z*)-vinylsilane product would be generated via **TS$_{JF}$** (Fig. 9b), which is only 6.8 kcal·mol$^{-1}$ higher in Gibbs energy than **J** (it has a relative energy of 3.6 kcal·mol$^{-1}$). This steps also regenerates the original catalytic species (**F**) upon coordination of a new hydrosilane molecule. Note that **TS$_{JF}$'**, which would lead to the β-(*E*)-vinylsilane product has a relative Gibbs energy of 11.8 kcal·mol$^{-1}$, that is, it is 8.2 kcal·mol$^{-1}$ less stable than **TS$_{JF}$**.

Overall, the catalytic cycle is highly endergonic, with ΔG = –38.4 kcal·mol$^{-1}$. The effective energy span for the whole cycle is 23.4 kcal·mol$^{-1}$, and is dictated by the Gibbs energy difference between **F** and **TS$_{FG}$**, [35] thus corresponding to the Cp*-assisted hydrosilane activation. Noteworthy, the proposed reaction mechanism is also consistent with the fact that no reaction of the catalyst with either alkyne or hydrosilane alone was observed. Namely, the reaction of **F** with HSiMe$_2$Ph yields a relatively unstable reaction intermediate (**H**, which is 11.3 kcal·mol$^{-1}$ higher in Gibbs energy). In this way, only the reaction with the alkyne displaces the reaction towards the products, allowing it to proceed.

We note that the energy span associated with this reaction mechanism is higher than that of the pathway operative in the presence of acetone, consistent with the experimentally observed faster reaction rate under the latter conditions. Accordingly, in the absence of acetone as solvent, the reaction is predicted to proceed through a pentamethylcyclopentadienyl-assisted mechanism, which, to the best of our knowledge, is unprecedented in this type of catalytic process.

A $^1$H NMR kinetic study of the hydrosilylation of phenylacetylene with HSiMe$_2$Ph and DSiMe$_2$Ph was also carried out. Experiments performed in CDCl$_3$ revealed a kinetic isotope effect (KIE) of 2.29, indicating that hydrosilane activation is involved in the rate-determining step in the absence of acetone, in agreement with the proposed mechanism. In contrast, no KIE was observed when the reaction was

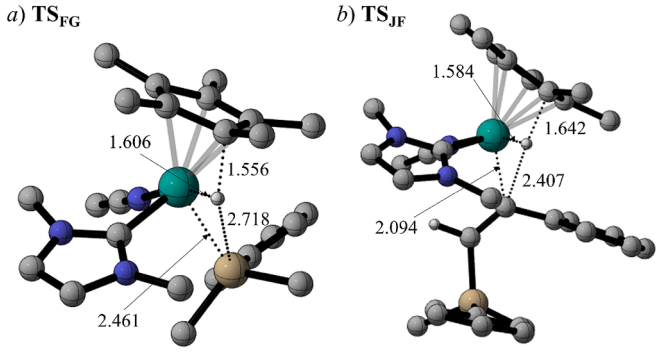


**Fig. 9.** DFT-optimized structures and selected distances of *a*) **TS$_{FG}$**, *b*) **TS$_{JF}$**. Non-essential hydrogen atoms have been omitted for clarity.

conducted in acetone-$d_6$ (see the Supporting Information); consistent with an outer-sphere ionic mechanism in which hydrosilane activation is not rate-determining.

At this point, it is worth noting that the calculated relative Gibbs energies of **$TS_{DE}$** and **$TS_{EA}$**, both identified as potentially rate-determining transition states, are essentially identical. On this basis, some degree of KIE might be expected, since **$TS_{EA}$** involves a hydrogen transfer from Rh, which proceeds from the hydrosilane. However, the computational methodology cannot distinguish between two transition states that are likely very close in Gibbs energy. To further assess this issue, a single-point calculation using the M06L functional—previously shown by some of us to accurately predict KIE effects in related systems [36]—was performed. The calculations indicate that $TS_{DE}$ is slightly higher in Gibbs energy than **$TS_{EA}$** (by 0.3 kcal·mol$^{-1}$), in line with our previous analysis. Accordingly, the experimental KIE supports **$TS_{DE}$** as the turnover-limiting transition state.

Overall, the KIE experiments are consistent with the proposed mechanistic picture and clearly demonstrate that distinct reaction mechanisms operate in $CDCl_3$ and acetone-$d_6$.

## 3. Experimental

### 3.1. General considerations

All reactions were carried out with rigorous exclusion of air using Schlenk-tube techniques or glovebox. Organic solvents were dried by standard methods and distilled under argon prior to use or obtained oxygen- and water-free from a Solvent Purification System (Innovative Technologies). The starting materials $[Cp^*RhI_2]_2$ [37] and $[Cp^*RhCl_2]_2$, [38] the imidazolium salts $[(MeImH)_2CH_2]I_2$ [39] and [IMeH]I, [40] and the salt $[HNEt_3]PF_6$ [41] were prepared as previously described in the literature. Compound $[Cp^*RhI\{(MeIm)_2CH_2\}]PF_6$ (**1**) was prepared following the procedure recently reported by us [23]. Deuterated solvents (Euriso-top) $CDCl_3$ and acetone-$d_6$ were dried using activated molecular sieves. The alkynes and hydrosilanes were obtained from commercial sources and used as received without further purification.

### 3.2. Scientific Equipment

C, H, and N analyses were carried out in a PerkinElmer 2400 Series II CHNS/O analyzer. $^1H$ and $^{13}C\{^1H\}$ NMR spectra were recorded on a Bruker Avance 300 (300.1278 MHz) or Bruker ARX-300 (300.130 MHz). Chemical shifts are reported in ppm relative to tetramethylsilane and coupling constants ($J$) are given in Hertz (Hz). High-resolution electrospray ionization mass spectra (HRMS-ESI) were recorded using a Bruker MicroToF-Q equipped with an API-ESI source and a Q-ToF mass analyzer, which leads a maximum error in the measurement of 5 ppm, using sodium formate as reference.

### 3.3. Synthesis of $[Cp^*Rh(NCCH_3)\{(MeIm)_2CH_2\}](PF_6)_2$ (2)

$AgPF_6$ (36.8 mg, 0.146 mmol) was added to a solution of $[Cp^*RhI\{(MeIm)_2CH_2\}]PF_6$ (**1**) (100 mg, 0.146 mmol) in acetonitrile (10 mL). The suspension was stirred at room temperature in the absence of light for 3 h, filtered through celite to remove the silver iodide formed, and washed with acetonitrile (2 x 2 mL). The solution was brought to dryness under vacuum to give an oily residue which was disaggregated by stirring with cold diethyl ether. The yellow solid was filtered, washed with diethyl ether (2 x 3 mL) and dried under vacuum. The solid was dissolved in acetonitrile (5 mL) and layered with diethyl ether (20 mL) to give a microcrystalline yellow solid which was filtered, washed with diethyl ether (3 x 2 mL) and dried in vacuo. Yield: 92 mg, 85 %. Anal. Calcd. for $C_{21}H_{30}F_{12}N_5P_2Rh$: C, 33.84; H, 4.06; N, 9.40. Found: C, 34.05; H, 4.23; N, 9.31. HRMS (ESI+, MeOH, $m/z$): calcd for $C_{19}H_{26}N_4Rh$ 413.1207 $[M-NCCH_3-H]^+$; found, 413.1244. $^1H$ NMR (300 MHz, acetone-$d_6$, 298 K): $\delta$ 7.72 (d, $J_{H\text{-}H}$ = 2.0, 2H, =CH Im), 7.63 (d, $J_{H\text{-}H}$ = 2.0, 2H, =CH Im), 6.61 (d, $J_{H\text{-}H}$ = 13.8, 1H, $NCH_2N$), 5.96 (d, $J_{H\text{-}H}$ = 13.8, 1H, $NCH_2N$), 4.04 (s, 6H, $NCH_3$), 2.58 (s, 3H, $NCCH_3$), 1.97 (s, 15H, Cp*). $^{13}C\{^1H\}$ NMR (75 MHz, acetone-$d_6$, 298 K): $\delta$ 164.9 (d, $J_{C\text{-}Rh}$ = 49.0, $C_{NCN}$), 125.8, 124.7 (=CH Im), 102.9 (d, $J_{C\text{-}Rh}$ = 5.5, $CCH_3$ Cp*), 66.1 ($NCH_2N$), 38.1 ($NCH_3$), 9.8 ($CH_3$ Cp*), 3.8 ($NCCH_3$).

### 3.4. Synthesis of $[Cp^*RhI_2\{(MeIm)CH_2(MeImH\}][Cp^*RhI_3]$ (3)

$NEt_3$ (9.65 µl, 0.069 mmol) was added to a suspension of $[Cp^*RhI_2]_2$ (67.9 mg, 0.069 mmol) and $[(MeImH)_2CH_2]I_2$ (30 mg, 0.069 mmol) in acetonitrile (5 ml). The mixture was stirred for 48 h go give a dark red suspension. The suspension was filtered and the resulting solution was brought to dryness under vacuum. The solid was dissolved in dichloromethane (1 mL) and precipitated with pentane (10 mL) to give a microcrystalline dark red solid which was filtered, washed with pentane (3 x 2 mL) and dried in vacuo. Yield: 82 mg, 92 %. Anal. Calcd. for $C_{29}H_{43}I_5N_4Rh_2$: C, 27.04; H, 3.36; N, 4.35. Found: C, 27.94; H, 2.90; N, 4.50. HRMS (ESI+, $CH_3CN$, $m/z$): calcd for $C_{19}H_{28}I_2N_4Rh$, 668.9453 $[M]^+$; found, 668.9454; calcd for $C_{19}H_{27}IN_4Rh$, 541.0335 $[M-I-H]^+$; found, 541.0340. HRMS (ESI-, $CH_3CN$, $m/z$): calcd for $C_{10}H_{15}I_3Rh$, 618.7357 $[M]^-$; found, 618.7364. $^1H$ NMR (300 MHz, $CDCl_3$, 298 K): $\delta$ 10.20 (s, 1H, NCHN), 8.08 (ft, $J_{H\text{-}H}$ = 1.7, 1H, =CH Im), 7.78 (t, $J_{H\text{-}H}$ = 2.0, 1H, =CH Im), 7.49 (AB system, $J_{AB}$ = 13.5, 2H, $>CH_2$), 7.12 (ft, $J_{H\text{-}H}$ = 1.7, 1H, =CH Im), 7.09 (d, $J_{H\text{-}H}$ = 2.1, 1H, =CH Im), 4.08 (s, 3H, $NCH_3$), 4.06 (s, 3H, $NCH_3$), 2.06 (s, 15H, Cp* anion) 1.91 (s, 15H, Cp* cation). $^{13}C\{^1H\}$ NMR (75 MHz, $CDCl_3$, 298 K): $\delta$ 170.0 (d, $J_{C\text{-}Rh}$ = 58.6, $C_{NCN}$), (137.3 s, $C_{NCHN}$), 126.1, 123.9, 122.5, 123.4 (=CH Im), 98.1, 94.9 ($CCH_3$ Cp*), 63.0 ($NCH_2N$), 44.4, 37.2 ($NCH_3$), 11.8, 8.9 (Cp*).

### 3.5. Synthesis of $[Cp^*RhI_2(IMe)]$ (4)

$Ag_2O$ (37.5 mg, 0.162 mmol) was added to a solution of [IMeH]I (72.5 mg, 0.323 mmol) in dichloromethane (15 mL) and the suspension stirred for 5 h in the absence of light. Then, $[Cp^*RhCl_2]_2$ (100 mg, 0.162 mmol) was added and the mixture stirred for a further 15 h. The resulting suspension was filtered through celite and washed with dichloromethane (2 x 3 mL). The red solution was brought to dryness under vacuum to give an orange solid, which was dissolved in methanol (5 mL). The solution was treated with KI in excess (124.5 mg, 0.75 mmol) and stirred for 5 h. Then, the darkened solution was brought to dryness to give a dark red solid which was extracted with $CH_2Cl_2$ (2 x 3 mL). The resulting solution was brought to dryness and the residue washed with diethyl ether (3 x 3 mL) and dried under vacuum. Yield: 154 mg, 81 %. Anal. Calcd. for $C_{15}H_{23}I_2N_2Rh$: C, 30.64; H, 3.94; N, 4.76. Found: C, 30.28; H, 3.51; N, 4.68. HRMS (ESI+, MeOH, $m/z$): calcd for $C_{15}H_{23}IN_2Rh$, 460.9956 $[M-I]^+$; found, 460.9918. $^1H$ NMR (300 MHz, $CDCl_3$, 298 K): $\delta$ 7.02 (s, 2H, =CH Im), 4.04 (s, 6H, $NCH_3$), 1.90 (s, 15H, Cp*). $^{13}C\{^1H\}$ NMR (298 K, $CDCl_3$): $\delta$ 166.7 (d, $J_{C\text{-}Rh}$ = 47.4, $C_{NCN}$), 124.4 (=CH Im), 96.9 ($CCH_3$ Cp*), 44.3 ($NCH_3$), 11.1 (Cp*).

### 3.6. Synthesis of $[Cp^*Rh(NCCH_3)_2(IMe)][BF_4]_2$ (5)

$AgBF_4$ (66.2 mg, 0.340 mmol) was added to a solution of **4** (100 mg, 0.170 mmol) in acetonitrile (10 mL) and the suspension stirred for 5 h in the absence of light. The clearest resulting suspension was filtered through celite and washed with acetonitrile (2 x 3 mL). The yellow solution was brought to dryness under vacuum to give a yellow oil which was disaggregated by stirring vigorously with pentane. The resulting yellow solid was washed with pentane (3 x 3 mL) and dried under vacuum. Yield: 78 mg, 78 %. Anal. Calcd. for $C_{19}H_{29}B_2F_8N_4Rh$, 590.1505: C, 38.68; H, 4.95; N, 9.50. Found: C, 38.19; H, 4.92; N, 9.17. HRMS (ESI+, $NCCH_3$, $m/z$): calcd for $C_{19}H_{29}N_4Rh$, 416.1447 $[M]^+$; calcd for $C_{17}H_{26}N_3Rh$, 375.1182 $[M-NCCH_3]^+$; found 375.2534; calcd for $C_{15}H_{24}N_2Rh$, 334.0916 $[M-2NCCH_3+H]^+$; found, 335.0984. $^1H$ NMR (300 MHz, $CD_3CN$, 298 K): $\delta$ 7.36 (s, 2H, =CH Im), 3.70 (s, 6H, $NCH_3$), 2.14 (s, 6H, $NCCH_3$),1.69 (s, 15H, Cp*). $^{13}C\{^1H\}$ NMR (298 K,

$CD_3CN$): $\delta$ 180.2 (d, $J_{C\text{-}Rh}$ = 42.3, $C_{NCN}$), 125.7 (=CH Im), 134.2 ($NCCH_3$), 101.6 (d, $J_{C\text{-}Rh}$ = 6.7, $CCH_3$ Cp*), 38.0 ($NCH_3$), 8.9 (Cp*), 0.4 ($NCCH_3$).

### 3.7. General procedure for catalytic alkyne hydrosilylation reactions

Hydrosilylation catalytic tests were carried out in NMR tubes under an argon atmosphere in acetone-$d_6$. In a typical procedure, an NMR tube was charged with the catalyst (1.1 x $10^{-3}$ mmol, 1 mol%), acetone-$d_6$ (0.4 mL), anisole (9.0 $10^{-3}$ mmol) as internal standard and the corresponding alkyne (0.110 mmol) and hydrosilane (0.110 mmol). The solution was kept at room temperature (298 K) and monitored by $^1$H NMR spectroscopy. Yields and selectivities were calculated by $^1$H NMR spectroscopy. The reaction products were unambiguously characterized on the basis of the $^3J_{H\text{-}H}$ coupling constants of the vinylic protons in the $^1$H NMR spectra and subsequent comparison to literature values (see the Supporting Information). Values for $J$ ranged from 17 to 19 Hz for β-(*E*), 13 to 16 Hz for β-(*Z*), and 1 to 3 Hz for α-vinylsilanes.

### 3.8. Procedure for gram-scale experiment

A Schlenk tube was charged with catalyst **4** (8.9 mg, 0.015 mmol, 0.25 mol%), acetone (5 mL), phenylacetylene (6.0 mmol, 672 μL), and $HSiMe_2Ph$ (6.0 mmol, 939 μL). The reaction mixture was stirred at room temperature for 4 h. The resulting yellow solution was passed through a short silica gel column, and removal of hexane (eluent) afforded dimethyl(phenyl)(*Z*-styryl)silane as a colourless liquid (1.22 g, 91 %).

### 3.9. Crystal structure determination

X-ray diffraction data of **3** and **4** were collected at 100(2) K on an APEX Bruker diffractometer with graphite-monochromated Mo − Kα radiation (λ = 0.71073 Å) using ω-scans. X-ray diffraction data of **5** were collected at 301(2) K on a D8 VENTURE diffractometer with graphite-monochromated Mo − Kα radiation (λ = 0.71073 Å) using ω-and ϕ-scans. Intensities were integrated and corrected for absorption effects with SAINT–PLUS [42] and SADABS [43] programs, both included in APEX4 package. The structures were solved by the Patterson method with SHELXS-9 [44] and refined by full matrix least-squares on F2 with SHELXL-2014 [45] under WinGX. [46] Pitch and yaw angles have been calculated according to the literature. [47].

### 3.10. Computational details

DFT calculations were performed with the Gaussian16 software package. [48] We selected the B3LYP exchange–correlation functional, [49] with D3BJ dispersion corrections. [50] Geometry optimizations were carried out using Ahlrichs def2-SVP double-zeta basis set, electronic energy results being further refined by means of single point calculations with triple-zeta def2- TZVP basis sets. [51] In all cases, an *"ultrafine"* integration grid was considered. Besides, we applied a PCM implicit solvation model (acetone), which we included in both gradients and energy calculations. [52] The nature of the stationary points was confirmed by analytical frequency analysis. We removed the translational entropy contribution to the Gibbs energy as proposed by Morokuma and co-workers. [53] Structure graphical representations were made by means of CylView software. [54].

## 4. Conclusions

Experimental studies on the residual hydrosilylation catalytic activity of compound $[Cp^*RhI\{(MeIm)_2CH_2\}]^+$ have led to the identification and characterization of the cationic species $[Cp^*RhI_2\{(MeIm)CH_2(MeImH)\}]^+$ as the active species, which is present at trace levels in uncrystallized samples. This study provided the basis for the rational redesign of the catalyst as $[Cp^*RhI_2(IMe)]$ (IMe = 1,3-dimethylimidozol-2-ylidene) and its application in the hydrosilylation of a series of terminal alkynes in acetone-$d_6$ at room temperature using $HSiMe_2Ph$ as hydrosilane. The hydrosilylation of ring-substituted phenylacetylene derivatives, linear aliphatic 1-alkynes and aliphatic and aromatic diynes proceeded efficiently to selectively afford the corresponding β-(*Z*)-vinylsilane derivatives in short reaction times. *O*-functionalized aliphatic terminal alkynes were well tolerated by the catalyst, whereas *N*-functionalized alkynes were not.

The mechanism of the hydrosilylation of phenylacetylene with $HSiMePh_2$ catalyzed by $[Cp^*RhI_2(IMe)]$ has been studied by DFT calculations. In acetone, the reaction is expected to proceed through an ionic outer-sphere mechanism, involving heterolytic activation of the hydrosilane assisted by the rhodium center and a molecule of solvent that acts as a silane-shuttle. However, in the absence of acetone, a novel reaction pathway based on metal–ligand cooperation is proposed. Within this mechanism, the metallocene moiety of $[Cp^*RhI_2(IMe)]$ is involved in the activation of the H–Si bond of the hydrosilane. The hydrosilane might be activated through a cooperative interaction with the Cp* ligand leading to the formation of a reactive Rh(I)–silyl intermediate with a pentamethylcyclopenta-1,3-diene ligand, [$\eta^4$-Cp*H], resulting from the protonation of the Cp* moiety. The observed β-(*Z*) selectivity arises from a metal-assisted isomerization of the initially formed (*Z*)-silylvinylene intermediate into the thermodynamically more stable (*E*)-silylvinylene species, via a metallacyclopropene intermediate, followed by proton transfer from the [$\eta^4$-Cp*H] ligand. The proposed mechanisms are consistent with the activity and selectivity exhibited by the catalyst in both solvents, as well as with KIE experiments. Moreover, we highlight the versatility and non-innocent nature of the Cp* ligand, which could inspire the design of new catalysts featuring this functionality.

## CRediT authorship contribution statement

**Isabel Poves-Ruiz:** Methodology, Investigation. **Beatriz Sánchez-Page:** Methodology, Investigation. **M. Victoria Jiménez:** Writing – review & editing, Validation, Supervision, Investigation, Conceptualization. **Miguel Gallegos:** Investigation, Data curation. **Julen Munarriz:** Writing – review & editing, Funding acquisition, Formal analysis, Data curation. **Vincenzo Passarelli:** Writing – review & editing, Formal analysis, Data curation. **Jesús J. Pérez-Torrente:** Writing – review & editing, Writing – original draft, Validation, Funding acquisition.

## Declaration of competing interest

The authors declare that they have no known competing financial interests or personal relationships that could have appeared to influence the work reported in this paper.

## Acknowledgements

The authors express their appreciation for the financial support from the Spanish Ministerio de Ciencia, Innovación y Universidades, MICIU/AEI/10.13039/501100011033, under the projects PID2022-137208NB-I00 and PID2024-159030NA-I00, as well as the "Departamento de Ciencia, Universidad y Sociedad del Conocimiento del Gobierno de Aragón" (group E42_23R). Authors would like to acknowledge the use of the Servicio General de Apoyo a la Investigación-SAI at the Universidad de Zaragoza, the scientific-technical services of the ISQCH/CEQMA (CSIC) and the Instituto de Biocomputación y Física de Sistemas Complejos (BIFI, Universidad de Zaragoza) for computational resources. We also thank Pilar García-Orduña for data collection and analysis of the X-ray structure of compound **5**.

## Appendix A. Supplementary data

Supplementary data to this article can be found online at https://doi.org/10.1016/j.jcat.2026.116721.

## Data availability

Data will be made available on request.

## References


[1] (a) T.T. Hiyama, M. Oestreich, Organosilicon Chemistry: Novel Approaches and Reactions, Weinheim, Wiley-VCH, 2019;
(b) V.Y. Lee, Organosilicon Compounds: From Theory to Synthesis to Applications, Elsevier, Amsterdam, 2017.

[2] (a) B. Marciniec, H. Maciejewski, C. Pietraszuk, P. Pawluć, Hydrosilylation and related reactions of silicon compounds, in: B. Cornils, W.A. Herrmann, M. Beller, R, R. Paciello (Eds.), Applied Homogeneous Catalysis with Organometallic Compounds, Wiley-VCH, Weinheim, Germany, 2017, pp. 569–620;
(b) B. Marciniec, H. Maciejewski, C. Pietraszuk, P. Pawluć, Hydrosilylation of alkenes and their derivatives, in: B. Marciniec (Ed.), Hydrosilylation: A Comprehensive Review on Recent Advances, Springer, Berlin, 2009, pp. 3–51;
(c) I. Ojima, Z. Li, J. Zhu, Recent advances in the hydrosilylation and related reactions, in: Z. Rappoport, Y. Apeloig (Eds.), The Chemistry of Organic Silicon Compounds vol. 2, Wiley, New York, 1998, pp. 1687–1792.

[3] (a) T. Komiyama, Y. Minami, T. Hiyama, Recent advances in transition-metal-catalyzed synthetic transformations of organosilicon reagents, ACS Catal. 7 (2017) 631–651;
(b) J. Szudkowska-Frątczak, G. Hreczycho, P. Pawluć, Silylative coupling of olefins with vinylsilanes in the synthesis of functionalized alkenes, Org. Chem. Front. 2 (2015) 730–738;
(c) Y. Nakao, T. Hiyama, Silicon-based cross-coupling reaction: an environmentally benign version, Chem. Soc. Rev. 40 (2011) 4893–4901;
(d) T.-Y. Luh, S.-T. Li, Synthetic applications of allylsilanes and vinylsilanes, in: Z. Rappoport, Y. Apeloig (Eds.), The Chemistry of Organic Silicon Compounds, vol. 2, John Wiley & Sons Inc, New York, 1999, pp. 1793–1868;
(e) B. Marciniec (Ed.), Comprehensive Handbook on Hydrosilylation, Pergamon Press, New York, 1992.

[4] B. Marciniec, Hydrosilylation of alkynes and their derivatives, in: Hydrosilylation: A Comprehensive Review on Recent Advances; B. Marciniec, Advances In Silicon Science, vol 1, Springer, Dordrecht, 2009, pp. 53–86.

[5] (a) P. He, M.-Y. Hu, X.-Y. Zhang, S.-F. Zhu, Transition-metal-catalyzed stereo- and regioselective hydrosilylation of unsymmetrical alkynes, Synthesis 54 (2022) 49–66;
(b) B.M. Trost, Z.T. Ball, Addition of metalloid hydrides to alkynes: hydrometallation with boron, silicon, and tin, Synthesis (2005) 853–887.

[6] (a) K. Chen, H. Zhu, Y. Li, Q. Peng, Y. Guo, X. Wang, Dinuclear cobalt complex-catalyzed stereodivergent semireduction of alkynes: switchable selectivities controlled by $H_2O$, ACS Catal. 11 (2021) 13696–13705;
(b) M.-Y. Hu, J. Lian, W. Sun, T.-Z. Qiao, S.-F. Zhu, Iron-catalyzed dihydrosilylation of alkynes: efficient access to geminal bis(silanes), J. Am. Chem. Soc. 141 (2019) 4579–4583;
(c) C.H. Jun, R.H. Crabtree, Dehydrogenative silation, isomerization, and the control of syn- vs anti-addition in the hydrosilation of alkynes, J. Organomet. Chem. 447 (1993) 177–187.

[7] (a) L. Mirghaffari, S. Hosseininezhad, M. Seydi, A. Ramazani, H. Ahankar, G. Zhang, Recent progress of platinum and rhodium catalysts in hydrosilylation reactions. Chem. Select, 10 (2025), 202501079; (b) M. Iglesias, F.J. Fernández-Álvarez, L.A. Oro, State of the art in rhodium- and iridium-catalyzed hydrosilylation reactions, in: Perspectives of Hydrosilylation Reactions, Marciniec, B., Maciejewski, H., Eds.; Topics in Organometallic Chemistry; Springer Nature: Cham, 2023; Vol. 72, pp 95–140.

[8] (a) L. Cerquera-Montealegre, D. Gallego, E.A. Baquero, Recent advances in the catalytic applications of NHC-early abundant metals (Mn Co, Fe) complexes, Adv. Organomet. Chem. 81 (2024) 1–28;
(b) R.R. Behera, R. Saha, A.A. Kumar, S. Sethi, N.C. Jana, B. Bagh, Hydrosilylation of terminal alkynes catalyzed by an air-stable manganese-NHC complex, J. Org. Chem. 88 (2023) 8133–8149;
(c) W. Bai, J. Sun, D. Wang, S.-D. Bai, L. Deng, Low-coordinate Cobalt(0) N-heterocyclic carbene complexes as catalysts for hydrosilylation of alkynes, Appl. Organomet. Chem. 36 (2022);
(d) J.-W. Park, Cobalt-catalyzed alkyne hydrosilylation as a new frontier to selectively access silyl-hydrocarbons, Chem. Commun. 58 (2022) 491–504;
(e) D. Wang, Y. Lai, P. Wang, X. Leng, J. Xiao, L. Deng, Cobalt-catalyzed regiodivergent hydrosilylation of internal alkynes: ligand-controlled access to α- and β-vinylsilanes, J. Am. Chem. Soc. 143 (2021) 12847–12856;
(f) Y. Gao, L. Wang, L. Deng, Distinct catalytic performance of Cobalt(I)–N-heterocyclic carbene complexes in hydrosilylation of alkenes and alkynes, ACS Catal. 8 (2018) 9637–9646.

[9] (a) G. Berthon-Gelloz, J.-M. Schumers, G. De Bo, I.E. Markó, Highly β-e)-selective hydrosilylation of terminal and internal alkynes catalyzed by a (IPr)Pt(Diene) complex, J. Org. Chem. 73 (2008) 4190–4197;
(b) I.E. Markó, S. Stérin, O. Buisine, G. Mignani, P. Branlard, B. Tinant, J.-P. Declercq, Selective and efficient platinum(0)-carbene complexes as hydrosilylation catalysts, Science 298 (2002) 204–206.

[10] (a) M.O. Karataş, B. Alıcı, V. Passarelli, I. Özdemir, J.J. Pérez-Torrente, R. Castarlenas, Iridium(I) complexes bearing hemilabile coumarin-functionalised N-heterocyclic carbene ligands with application as alkyne hydrosilylation catalysts, Dalton Trans. 50 (2021) 11206–11215;
(b) B. Sánchez-Page, M.V. Jiménez, J.J. Pérez-Torrente, V. Passarelli, J. Blasco, G. Subias, M. Granda, P. Álvarez, Hybrid catalysts comprised of graphene modified with rhodium-based N-heterocyclic carbenes for alkyne hydrosilylation, ACS Appl. Nano Mater. 3 (2020) 1640–1655;
(c) A. Zanardi, E. Peris, J.A. Mata, Alkenyl-functionalized NHC iridium-based catalysts for hydrosilylation, New J. Chem. 32 (2008) 120–126.

[11] (a) M.C. Cassani, M.A. Brucka, C. Femoni, M. Mancinelli, A. Mazzanti, R. Mazzoni, G. Solinas, N-heterocyclic carbene rhodium(I) complexes containing an axis of chirality: dynamics and catalysis, New J. Chem. 38 (2014) 1768–1779;
(b) L. Busetto, M.C. Cassani, C. Femoni, M. Mancinelli, A. Mazzanti, R. Mazzoni, G. Solinas, N-heterocyclic carbene-amide rhodium(I) complexes: structures, dynamics, and catalysis, Organometallics 30 (2011) 5258–5272;
(c) M.V. Jiménez, J.J. Pérez-Torrente, M.I. Bartolomé, V. Gierz, F.J. Lahoz, L. A. Oro, Rhodium(I) complexes with hemilabile N-heterocyclic carbenes: efficient alkyne hydrosilylation catalysts, Organometallics 27 (2008) 224–234.

[12] (a) A. Tyagi, S. Yadav, P. Daw, C. Ravi, J.K. Bera, A Rh(I) complex with an annulated N-heterocyclic carbene ligand for E-selective alkyne hydrosilylation, Polyhedron 172 (2019) 167–174;
(b) J.P. Morales-Cerón, P. Lara, J. López-Serrano, L.L. Santos, V. Salazar, E. Álvarez, A. Suárez, Rhodium(I) complexes with ligands based on N-heterocyclic carbene and hemilabile pyridine donors as highly E stereoselective alkyne hydrosilylation catalysts, Organometallics 36 (2017) 2460–2469.

[13] (a) M. González-Laínez, M.V. Jiménez, V. Passarelli, J.J. Pérez-Torrente, β-(Z)-selective alkyne hydrosilylation by a N, O-functionalized NHC-based rhodium(I) catalyst, Dalton Trans. 52 (2023) 11503–11517;
(b) E. Mas-Marzá, M. Sanaú, E. Peris, Coordination versatility of pyridine-functionalized N-heterocyclic carbenes: a detailed study of the different activation procedures. Characterization of new Rh and Ir compounds and study of their catalytic activity, Inorg. Chem. 44 (2005) 9961–9967.

[14] (a) R.H. Lam, S.T. Keaveney, B.A. Messerle, I. Pernik, Bimetallic rhodium complexes: precatalyst activation-triggered bimetallic enhancement for the hydrosilylation transformation, ACS Catal. 13 (2023) 1999–2010;
(b) D. Rendón-Nava, J.M. Vásquez-Pérez, C.I. Sandoval-Chávez, A. Álvarez-Hernández, D. Mendoza-Espinosa, Synthesis of multinuclear Rh(I) complexes bearing triazolylidenes and their application in C-C and C–Si bond forming reactions, Organometallics 39 (2020) 3965–3974;
(c) G. Mancano, M.J. Page, M. Bhadbhade, B.A. Messerle, Hemilabile and bimetallic coordination in Rh and Ir complexes of NCN pincer ligands, Inorg. Chem. 53 (2014) 10159–10170.

[15] (a) S. Dierick, E. Vercruysse, G. Berthon-Gelloz, I.E. Markó, User-friendly platinum catalysts for the highly stereoselective hydrosilylation of alkynes and alkenes, Chem. Eur. J. 21 (2015) 17073–17078;
(b) G. De Bo, G. Berthon-Gelloz, B. Tinant, I.E. Markó, Hydrosilylation of alkynes mediated by N-heterocyclic carbene platinum(0) complexes, Organometallics 25 (2006) 1881–1890.

[16] (a) R.S. Tanke, R.H. Crabtree, Unusual activity and selectivity in alkyne hydrosilylation with an iridium catalyst stabilized by an oxygen-donor ligand, J. Am. Chem. Soc. 112 (1990) 7984–7989;
(b) I. Ojima, N. Clos, R.J. Donovan, P. Ingallina, Hydrosilylation of 1-hexyne catalyzed by rhodium and cobalt-rhodium mixed-metal complexes, mechanism of apparent trans addition, Organometallics 9 (1990) 3127–3133.

[17] S. Vásquez-Céspedes, X. Wang, F. Glorius, Plausible Rh(V) intermediates in catalytic C-H activation reactions, ACS Catal. 8 (2018) 242–257.

[18] (a) T.T. Metsänen, P. Hrobárik, H.F.T. Klare, M. Kaupp, M. Oestreich, Insight into the mechanism of carbonyl hydrosilylation catalyzed by Brookhart's cationic iridium(III) pincer complex, J. Am. Chem. Soc. 136 (2014) 6912–6915;
(b) V.S. Sridevi, Y.F. Wai, K.L. Weng, Stereoselective hydrosilylation of terminal alkynes catalyzed by $[Cp^*IrCl_2]_2$: a computational and experimental study, Organometallics 26 (2007) 1157–1160;
(c) V. Comte, C. Balan, P. Le Gendre, C. Moïse, From inconsistent results to high speed hydrosilylation, Chem. Commun. 17 (2007) 713–715;
(d) H. Nagashima, K. Tatebe, T. Ishibashi, A. Nakaoka, J. Sakakibara, K. Itoh, Unusual rate enhancement in the $RhCl(PPh_3)_3$-catalyzed hydrosilylation by organosilanes having two Si–H groups at appropriate distances: mechanistic aspects, Organometallics 14 (1995) 2868–2879;
(e) S.B. Duckett, R.N. Perutz, Mechanism of homogeneous hydrosilation of alkenes by (η5-cyclopentadienyl)rhodium, Organometallics 11 (1992) 90–98.

[19] (a) M. Roemer, S.T. Keaveney, V.R. Gonçales, J. Lian, J.E. Downes, S. Gautam, J. J. Gooding, B.A. Messerle, Engineering regioselectivity in the hydrosilylation of alkynes using heterobimetallic dual-functional hybrid catalysts, Catal. Sci. Technol. 12 (2022) 226–236;
(b) X. Zhao, D. Yang, Y. Zhang, B. Wang, J. Qu, Highly β(Z)-selective hydrosilylation of terminal alkynes catalyzed by thiolate-bridged dirhodium complexes, Org. Lett. 20 (2018) 5357–5361;
(c) M. Navarro, C.A. Smith, M. Albrecht, Enhanced catalytic activity of iridium(III) complexes by facile modification of C, N-bidentate chelating pyridylideneamide ligands, Inorg. Chem. 56 (2017) 11688–11701;
(d) J.J. Pérez-Torrente, D.H. Nguyen, J.M. Jiménez, F.J. Modrego, R. Puerta-Oteo, D. Gómez-Bautista, M. Iglesias, L.A. Oro, Hydrosilylation of terminal alkynes catalyzed by a ONO-pincer iridium(III) hydride compound: mechanistic insights into the hydrosilylation and dehydrogenative silylation catalysis, Organometallics 35 (2016) 2410–2422;
(e) Y. Corre, C. Werlé, L. Brelot-Karmazin, J.-P. Djukic, F. Agbossou-Niedercorn, C. Michon, Regioselective hydrosilylation of terminal alkynes using pentamethylcyclopentadienyl iridium(III) metallacycle catalysts, J. Mol. Catal. A: Chem. 423 (2016) 256–263;

(f) M. Iglesias, M. Aliaga-Lavrijsen, P.J.S. Miguel, F.J. Fernández-Álvarez, J. J. Pérez-Torrente, L.A. Oro, Preferential α-hydrosilylation of terminal alkynes by Bis-N-heterocyclic carbene rhodium(III) catalysts, Adv. Synth. Catal. 357 (2015) 350–354.

[20] (a) P.K.R. Panyam, B. Atwi, F. Ziegler, W. Frey, M. Nowakowski, M. Bauer, M. R. Buchmeiser, Rh(I)/(III)-N-heterocyclic carbene complexes: effect of steric confinement upon immobilization on regio- and stereoselectivity in the hydrosilylation of alkynes, Chem. – Eur. J. 27 (2021) 17220–17229;
(b) E. van Vuuren, F.P. Malan, W. Cordier, M. Nell, M. Landman, Self-isomerized–cyclometalated rhodium NHC complexes as active catalysts in the hydrosilylation of internal alkynes, Organometallics 41 (2022) 187–200;
(c) L. Ge, T. Li, Y. Duan, R. Feng, S. Guo, [C^{CC}]-type pincer carbene complexes of rhodium(III): synthesis and catalytic applications, Appl. Organomet. Chem. 39 (2025) e7825.

[21] M. Iglesias, P.J. Sanz Miguel, V. Polo, F.J. Fernández-Alvarez, J.J. Pérez-Torrente, L.A. Oro, An alternative mechanistic paradigm for the β-Z hydrosilylation of terminal alkynes: the role of acetone as a silane shuttle, Chem. Eur. J. 19 (2013) 17559–17566.

[22] B. Sánchez-Page, J. Munarriz, M.V. Jiménez, J.J. Pérez-Torrente, J. Blasco, G. Subias, V. Passarelli, A. Álvarez, β-(Z) selectivity control by cyclometalated rhodium(III)−triazolylidene homogeneous and heterogeneous terminal alkyne hydrosilylation catalysts, ACS Catal. 10 (2020) 13334–13351.

[23] R. Puerta-Oteo, J. Munarriz, V. Polo, M.V. Jiménez, J.J. Pérez-Torrente, Carboxylate assisted β-(Z) stereoselective hydrosilylation of terminal alkynes catalyzed by a zwitterionic Bis-NHC rhodium(III) complex, ACS Catal. 10 (2020) 7367–7380.

[24] (a) M. Viciano, M. Poyatos, M. Sanaú, E. Peris, A. Rossin, G. Ujaque, A. Lledós, C-H oxidative addition of bisimidazolium salts to iridium and rhodium complexes, and N-heterocyclic carbene generation. A combined experimental and theoretical study, Organometallics 25 (2006) 1120–1134;
(b) M. Vogt;, V. Pons, D.M. Heinekey, Synthesis and characterization of a dicationic dihydrogen complex of iridium with a bis-carbene ligand set, Organometallics 24 (2005) 1832–1836;
(c) M. Poyatos, E. Mas-Marzá, M. Sanaú, E. Peris, Synthesis and reactivity of new chelate-N-heterocyclic biscarbene complexes of ruthenium, Inorg. Chem. 43 (2004) 1793–1798;
(d) W.A. Herrmann, J. Schwarz, High-yield syntheses of sterically demanding bis (N-heterocyclic carbene) complexes of palladium, Organometallics 18 (1999) 4082–4089.

[25] W. Zhong, Z. Fei, R. Scopelliti, R.P. Dyson, Alcohol-induced C−N bond cleavage of cyclometalated N-heterocyclic carbene ligands with a methylene-linked pendant imidazolium ring, Chem. Eur. J. 22 (2016) 12138–12144.

[26] (a) P. Frisch, T. Szilvasi, S. Inoue, Facile access to dative, single, and double silicon−metal bonds through M−Cl insertion reactions of base-stabilized siii cations, Chem.– Eur. J. 26 (2020) 6271–6278;
(b) I. de Krom, L.E.E. Broeckx, M. Lutz, C. Muller, 2-(2′-Pyridyl)-4,6-diphenylphosphinine versus 2-(2′-Pyridyl)-4,6-diphenylpyridine: synthesis, characterization, and reactivity of cationic rhiii and iriii complexes based on aromatic phosphorus heterocycles, Chem.– Eur. J. 19 (2013) 3676–3684;
(c) G. Su, X.-K. Huo, G.-X. Jin, Half-sandwich Ru(II), Ir(III) and Rh(III) complexes with bridging or chelating N-heterocyclic bis-carbene ligand: Synthesis and characterization, J. Organomet. Chem. 696 (2011) 533–538;
(d) W.-G. Jia, Y.-B. Huang, Y.-J. Lin, G.-X. Jin, Syntheses and structures of half-sandwich iridium(III) and rhodium(III) complexes with organochalcogen (S, Se) ligands bearing N-methylimidazole and their use as catalysts for norbornene polymerization, Dalton Trans. 5612–5620 (2008);
(e) C. Pettinari, R. Pettinari, F. Marchetti, A. Macchioni, D. Zuccaccia, B. W. Skelton, A.H. White, Synthesis, reactivity, spectroscopic characterization, X-ray structures, PGSE, and NOE NMR studies of (η5-C5Me5)-rhodium and -iridium derivatives containing bis(pyrazolyl)alkane ligands, Inorg. Chem. 46 (2007) 896–906;
(f) D.F. Kennedy, B.A. Messerle, M.K. Smith, Synthesis of Cp* iridium and rhodium complexes containing bidentate sp2-N-donor ligands and counter-anions [Cp*MCl3]–, Eur. J. Inorg. Chem. 80–89 (2007);
(g) L. Quebatte, R. Scopelliti, K. Severin, Synthesis, structure and reactivity of homo- and heterobimetallic complexes of the general formula [Cp*Ru(μ-Cl)3ML] [LM = (arene)Ru, Cp*Rh, Cp*Ir], Eur. J. Inorg. Chem. 231–236 (2006).

[27] (a) T.T.Y. Tan, F.E. Hahn, Synthesis of Iridium(III) and Rhodium(III) complexes bearing C8-metalated theophylline ligands by directed C-H activation, Organometallics 38 (2019) 2250–2258;
(b) F. Aznarez, P.J.S. Miguel, T.T.Y. Tan, F.E. Hahn, Preparation of Rhodium(III) Di-NHC chelate complexes featuring two different NHC donors via a mild NaOAc-assisted C–H activation, Organometallics 35 (2016) 410–419.

[28] (a) C.M. Bernier, C.M. Du Chane, J.S. Martinez, J.O. Falkinham III, J.S. Merola, Synthesis, characterization, and antimicrobial activity of RhIII and IrIII N-heterocyclic carbene piano-stool complexes, Organometallics 40 (2021) 1670–1681;
(b) X.-Q. Xiao, G.-X. Jin, Half-sandwich rhodium complexes containing both N-heterocyclic carbene and ortho-carborane-1,2- dithiolate ligands, J. Organomet. Chem. 693 (2008) 316–320.

[29] $^1$H NMR data for [Cp*RhI(IMe)$_2$]I: δ $^1$H NMR (300 MHz, $CDCl_3$, 298 K): δ 6.99 (s, 2H, =CH Im), 6.98 (s, 2H, =CH Im), 4.07 (s, 6H, $NCH_3$), 3.98 (s, 6H, $NCH_3$), 1.76 (s, 15H, Cp*). HRMS (ESI+, MeOH, m/z): calcd for $C_{20}H_{31}IN_4Rh$, 557.0643 $[M]^+$; found, 557.0659.

[30] A. Pita-Milleiro, M.G. Alférez, J.J. Moreno, M.F. Espada, C. Maya, J. Campos, Unveiling the latent reactivity of Cp* Ligands ($C_5Me_5$) toward carbon nucleophiles on an iridium complex, Inorg. Chem. 62 (2023) 5961–5971.

[31] A. Zamorano, N. Rendón, J.E.V. Valpuesta, E. Álvarez, E. Carmona, Synthesis and reactivity toward $H_2$ of ($\eta^5$-$C_5Me_5$)Rh(III) complexes with bulky aminopyridinate ligands, Inorg. Chem. 54 (2015) 6573–6581.

[32] W.N.O. Wylie, A.J. Lough, R.H. Morris, Bifunctional mechanism with unconventional intermediates for the hydrogenation of ketones catalyzed by an Iridium(III) complex containing an N-heterocyclic carbene with a primary amine donor, Organometallics 31 (2012) 2152–2165.

[33] (a) L.M. Aguirre Quintana, S.I. Johnson, S.L. Corona, W. Villatoro, W.A. Goddard III, M.K. Takase, D.G. Van der Velde, J.R. Winkler, H.B. Gray, J.D. Blakemore, Proton–hydride tautomerism in hydrogen evolution catalysis. Proc. Natl. Acad. Sci. U. S. A. 2016, 113, 6409–6414; (b) C.L. Pitman, O.N.L. Finster, A.J.M. Miller, Cyclopentadiene-mediated hydride transfer from rhodium complexes. Chem. Commun. 2016, 52, 9105–9108; (c) C.E. Kefalidis, L. Perrin, C.J. Burns, D.J. Berg, L. Maron, R.A. Andersen, Can a pentamethylcyclopentadienyl ligand act as a proton-relay in f-element chemistry? Insights from a joint experimental/theoretical study. Dalton Trans. 2015, 44, 2575–2587.

[34] (a) M.J. Chalkley, P.H. Oyala, J.C. Peters, Cp* noninnocence leads to a remarkably weak C−H bond via metallocene protonation, J. Am. Chem. Soc. 141 (2019) 4721–4729;
(b) M.J. Chalkley, T.J. Del Castillo, B.D. Matson, J.C. Peters, Fe-Mediated nitrogen fixation with a metallocene mediator: exploring pKa Effects and demonstrating electrocatalysis, J. Am. Chem. Soc. 140 (2018) 6122–6129;
(c) M.J. Chalkley, T.J. Del Castillo, B.D. Matson, J.P. Roddy, J.C. Peters, Catalytic N2-to-NH3 conversion by Fe at lower driving force: a proposed role for metallocene-mediated PCET, ACS Cent. Sci. 3 (2017) 217–223.

[35] S. Kozuch, S. Shaik, How to conceptualize catalytic cycles? The energetic span model, Acc. Chem. Res. 44 (2011) 101–110.

[36] M. Galiana-Cameo, A. Urriolabeitia, E. Barrenas, V. Passarelli, J.J. Perez-Torrente, A. Di Giuseppe, V. Polo, R. Castarlenas, Metal–ligand cooperative proton transfer as an efficient trigger for rhodium-NHC-pyridonato catalyzed gem-specific alkyne dimerization, ACS Catal. 11 (2021) 7553–7567.

[37] I. Ojima, A.T. Vu, D. Bonafoux, Product Class 5: organometallic complexes of rhodium, Science of Synthesis 1 (2002) 531–616.

[38] C. White, A. Yates, P. M. Maitlis, D. M. Heinekey, ($\eta^5$-Pentamethylcyclopentadienyl)Rhodium and -Iridium Compounds. In Inorganic Syntheses; John Wiley & Sons, Inc, 1992; Vol. 29, pp 228– 234.

[39] C. Quezada, J.C. Garrison, C.A. Tessier, W.J. Youngs, Synthesis and structural characterization of two bis(imidazol-2-ylidene) complexes of Pt(II), J. Organomet. Chem. 671 (2003) 183–186.

[40] B.L. Benac, E.M. Burguess, A.J. Arduengo III, 1,3-Dimethylimidazole-2-thione [2H-Imidazole-2-thione, 1,3-dihydro-1,3-dimethyl-], Org. Syn. 64 (1986) 92.

[41] B.M. Trost, R.C. Livingston, An atom-economic and selective ruthenium-catalyzedredox isomerization of propargylic alcohols. An efficient strategy for the synthesis of leukotrienes, J. Am. Chem. Soc. 130 (2008) 11970–11978.

[42] SAINT+: Area-Detector Integration Software, version 6.01; Bruker AXS: Madison, WI, **2001**.

[43] G.M. Sheldrick, *SADABS program*, University of Göttingen, Göttingen, Germany, 1999.

[44] G.M. Sheldrick, *SHELXS 97*, Program for the Solution of Crystal Structure; University of Göttingen, Göttingen, Germany, 1997.

[45] G.M. Sheldrick, Crystal structure refinement with SHELXL, Acta Cryst., Sect. C Struct. Chem. 71 (2015) 3–8.

[46] L.J. Farrugia, WinGX and ORTEP for windows: an update, J. Appl. Cryst. 45 (2012) 849–854.

[47] R. Azpíroz, L. Rubio-Pérez, A. Di Giuseppe, V. Passarelli, F.J. Lahoz, R. Castarlenas, J.J. Pérez-Torrente, L.A. Oro, Rhodium(I)-N-heterocyclic carbene catalyst for selective coupling of N-vinylpyrazoles with alkynes via C–H activation, ACS Catal. 4 (2014) 4244–4253.

[48] M.J. Frisch, G.W. Trucks, H.B. Schlegel, G.E. Scuseria, M.A. Robb, J.R. Cheeseman, G. Scalmani, V. Barone, G.A. Petersson, H. Nakatsuji, et al. Gaussian 16, revision C.01; Gaussian, Inc.: Wallingford, CT, 2016.

[49] A.D. Becke, A new mixing of Hartree-Fock and local density functional theories, J. Chem. Phys. 98 (1993) 1372–1377.

[50] (a) S. Grimme, J. Antony, S. Ehrlich, H. Krieg, A consistent and accurate ab initio parametrization of density functional dispersion correction (DFT-D) for the 94 elements H-Pu, J. Chem. Phys. 132 (2010) 154104;
(b) E.R.E. Johnson, A.D. Becke, A post-Hartree-Fock model of intermolecular interactions, J. Chem. Phys. 123 (2005) 024101.

[51] F. Weigend, R. Ahlrichs, Balanced basis sets of split valence, triple zeta valence and quadruple zeta valence quality for H to Rn: design and assessment of accuracy, Phys. Chem. Chem. Phys. 7 (2005) 3297–3305.

[52] G. Scalmani, M.J. Frisch, Continuous surface charge polarizable continuum models of solvation. I. General formalism, J. Chem. Phys. 132 (2010) 114110.

[53] R. Tanaka, M. Yamashita, L.W. Chung, K. Morokuma, K. Nozaki, Mechanistic studies on the reversible hydrogenation of carbon dioxide catalyzed by an Ir-PNP complex, Organometallics 30 (2011) 6742–6750.

[54] CYLview, 1.0b; C. Y. Legault, Ed.; Université de Sherbrooke, 2009 (http://www.cylview.org).